PERGAMON

International Journal of Solids and Structures 40 (2003) 2535–2561

INTERNATIONAL JOURNAL OF SOLIDS and STRUCTURES

www.elsevier.com/locate/ijsolstr

Bifurcation phenomena in the rigid inclusion power law matrix composite sphere

Alan J. Levy *

Department of Mechanical, Aerospace and Manufacturing Engineering, Syracuse University, 151 Link Hall, Syracuse, NY 13244-1240, USA

Received 31 January 2002; received in revised form 24 December 2002

Abstract

Bifurcation of interface separation related to cavity nucleation is analyzed for a radially loaded composite sphere consisting of a rigid inclusion separated from a power law matrix by a uniform, non-linear cohesive zone. Equations for the spherically symmetric and non-symmetric problems are obtained from a hyperelastic finite strain theory by a limiting process that preserves non-linear matrix and interface response at infinitesimal strain. A complete solution to the symmetric problem is presented including bifurcation load, stresses, and evolution of elasto-plastic boundary and interface separation. An analysis of non-symmetric bifurcation, under symmetric conditions of geometry and loading, yields the bifurcation load and first non-symmetric mode shape associated with rigid inclusion displacement. An energy analysis is carried out for both symmetric and non-symmetric problems in order to assess stability of spherically symmetric states to spherically symmetric and non-symmetric "rigid body mode" perturbations.

Results are provided for an interface force law that captures interface failure in normal mode and linear response in shear mode. For the symmetric problem, (i) there are threshold parameter values above which bifurcation will generally not occur, (ii) threshold values below which there do not exist equilibria in the post bifurcation regime, (iii) bifurcation occurs after attainment of the maximum interface strength. For the non-symmetric problem, (i) bifurcation always occurs, although it can be delayed by interfacial shear, (ii) for the smooth interface, non-symmetric bifurcation occurs after attainment of the maximum interface strength and always precedes symmetric bifurcation.

Keywords: Bifurcation problem; Plasticity; Cavity nucleation; Interfacial debonding and decohesion; Inclusion problem

1. Introduction

Cavity nucleation in solid material is generally an ambiguous concept, precisely defined only in the narrow context of specific materials, problem geometries or solution methodologies. Thus, in early work on steel, cavity nucleation was seen to be an event associated with separation of an elastic inclusion from the

* Fax: +1-315-443-9099.
E-mail address: ajlevy@syr.edu (A.J. Levy).

0020-7683/03/$ - see front matter © 2003 Elsevier Science Ltd. All rights reserved.
doi:10.1016/S0020-7683(03)00053-2

generally plastic matrix. Critical loads to precipitate this event were typically determined based on (i) an energy balance (accounting for interface energy) (Tanaka et al., 1970), (ii) the attainment of a prescribed interfacial stress (Argon et al., 1975), (iii) a combination of (i) and (ii) (Fisher and Gurland, 1981b). These theories are ad hoc in the sense that they do not define what precisely happens after the attainment of the critical load, or they are not readily applicable to anything but the simplest geometries. In a groundbreaking paper, Needleman (1987) employed the finite element method to study the formation of a cavity at the interface between an elastic inclusion and a viscoplastic matrix utilizing a non-linear cohesive zone to affect separation. In that work, cavity nucleation was seen as a process beginning with initial debonding and ending with complete decohesion (vanishing of tractions across the interface). The stress–strain response for the composite system analyzed reveals brittle decohesion, i.e., the sudden stress drop at the inclusion matrix interface within a small interval of strain. Although Needleman does define criteria for cavity nucleation, these definitions are unrelated to the abrupt unloading of the interface. This is due to the fact that, because of the symmetry imposed in his formulation, the only critical event is brittle decohesion, which occurs for only a range of parameter values. The criteria suggested are either dependent on the constitutive model used to characterize the interface or, are inherently imprecise. For example, physically based exponentially decaying interface force laws always require that some traction act across the interface so a definition of nucleation based on complete interfacial decohesion would fail to predict nucleation. Alternatively, a definition based on initial separation would predict that nucleation would always occur at the onset of any applied load. Finally, a definition based on the equivalence of plastic volume strain for the composite system and a comparison voided system requires that one specify the value of plastic volume strain for equivalence (difficulties with this definition have been pointed out by Needleman (1987)). Probably motivated by the fact that cavities nucleate in steel specimens subject to small overall straining (Rogers, 1960; Hahn and Rosenfield, 1966; Cox and Low, 1974) all of the work referred to above (with the exception of Needleman (1987)) was carried out within an infinitesimal framework. The work of Needleman assumed finite strains although this fact is largely incidental to the basic phenomenon of nucleation, which can occur in an infinitesimal strain analysis as well since the seat of nucleation is the interface force-separation relation and not finite strain kinematics or even non-linear material response.

Cavity nucleation phenomena in rubber initiated with the work of Ball (1982) on bifurcation of equilibrium solutions in finite elasticity. The specific application of these results has been carried out for a number of spherically and rotationally symmetric geometric configurations and material assumptions with like symmetry constraints assumed to hold in the post bifurcation regime (Horgan and Polignone (1995) reviews this extensive body of work). Here cavity nucleation is an event coincident with bifurcation of equilibria and coincides with the sudden appearance of a cavity or, the instantaneous growth of a microvoid, in previously uniform material. In this context, nucleation is a fundamental material instability critically dependent on the finite strain framework. It is important to note that Chung et al. (1987) studied this phenomenon in a sphere of uniform material modeled by the J_2 flow theory of plasticity. The critical load that they obtain is unrealistically high although they do comment on the potential significance of stress concentrators, i.e., inclusions, in obtaining realistic critical loads. Furthermore, they note that bifurcation at finite load is not possible in the limit of infinitesimal strain plasticity.

The above discussion suggests that it is acceptable to consider the phenomenon of cavity nucleation in alloys and metal matrix composites within an infinitesimal strain framework provided the inclusion–matrix interface energy is small. When this is true the nucleation event, or the critical part of the nucleation process, occurs when the strains may still be regarded as everywhere infinitesimal. Furthermore, in the absence of rational definitions of cavity nucleation by interfacial separation, it is desirable to equate the nucleation event to bifurcation resulting from interface force-separation constitutive relations. This is because bifurcation points are unambiguous properties of a system and further, because bifurcation more often than not occurs at a state in the separation process that would be physically reasonable to identify with nucleation. This approach has been adopted by the author in a series of papers analyzing the bifur-

cation structure of equilibrium solutions in a simple inclusion–interface-matrix system assuming a smooth interface (Levy, 1997), assuming interfacial shear (Levy, 1998), and accounting for pair interactions (Levy and Hardikar, 1999). Essentially, it was found that symmetry-preserving bifurcations, which characterize brittle decohesion, exist only for a limited range of parameter values. However, symmetry-breaking bifurcations, which characterize ductile or brittle decohesion, are associated with the rigid displacement of the inclusion within the matrix cavity, and exist for all parameter values. Interfacial shear can delay symmetry breaking bifurcations but not eliminate them. Therefore, it makes sense to identify nucleation with symmetry-breaking bifurcation and to regard the critical load to initiate them as the nucleation load. In the work just cited, non-linearity was confined to the interfacial cohesive zone, and linear elastic constituents were assumed, the direct applicability of those results to metallic material systems was therefore limited. Recently, Levy (2001, 2002) considered the bifurcation of equilibrium interfacial separation in a finitely deformed cylindrical inclusion–unbounded matrix system (Levy, 2001) and in a finitely deformed composite sphere (Levy, 2002). The constituent materials were a rigid inclusion and an incompressible hyperelastic matrix. The analyses employed well-known radial or spherical symmetric fields to obtain the critical load for bifurcation to a symmetric mode, and the theory of infinitesimal strain superimposed on a given finite strain to obtain the critical load to initiate bifurcation to a non-symmetrical mode characterized by a rigid body displacement of the inclusion within the matrix cavity. These works confirm the validity of infinitesimal strain analysis for bifurcation at small interface energy.

In this paper, results applicable to metallic material systems are presented. Specifically, we utilize the theory developed in Levy (2002) to study bifurcation phenomena associated with inclusion–matrix interfacial separation in an *infinitesimally* deformed composite sphere composed of a rigid inclusion and a hyperelastic, power law material matrix. The goal is to obtain critical loads for symmetric and non-symmetric bifurcation, and related stress and deformation fields, from the finite strain theory by a formal limit process that preserves non-linear material and interface response at infinitesimal strain. The first part of the paper concerns the spherically symmetric bifurcation problem while the second treats aspects of the non-symmetric problem. In both parts, we present an energy analysis for stability, which is similar in some respects to that employed by Horgan and Pence (1989). Because of the limitations inherent in the theory of infinitesimal strain superimposed on a given finite strain, the energy analysis for the non-symmetric problem can only be used to assess stability of spherically symmetric equilibrium states to non-symmetric "rigid body mode" perturbations.

2. Spherically symmetric equilibrium states

2.1. Some results for the finite strain problem

The spherically symmetric problem of interfacial separation in a composite sphere composed of a rigid inclusion and power law material matrix may be solved by direct application of the equations governing infinitesimal strain plasticity. Here we eschew this approach in favor of appropriate linearization of the finite strain theory to obtain the response at infinitesimal strain. This indirect approach is very efficient when considering non-symmetrical solutions arising from bifurcation under spherically symmetric conditions of geometry and loading. Below we briefly present the relevant equations needed for the analysis including expressions for the potential energy of the composite sphere and its derivatives.

Consider a composite sphere B consisting of a rigid inclusion Ω embedded in an incompressible hyperelastic matrix shell $B-\Omega$. A Cartesian coordinate system with origin at the sphere center $\mathbf{o}$ has basis $(\mathbf{e}_1,\mathbf{e}_2,\mathbf{e}_3)$, material point coordinates (p_1,p_2,p_3) and place coordinates (x_1,x_2,x_3). We will need two spherical coordinate systems with origin at $\mathbf{o}$. One has physical basis $(\mathbf{e}_R,\mathbf{e}_\Theta,\mathbf{e}_\Phi)$, coordinates (R,Θ,Φ) and is associated with material points while the other has physical basis $(\mathbf{e}_r,\mathbf{e}_\theta,\mathbf{e}_\varphi)$, coordinates (r,θ,φ) and is

associated with places. They are oriented such that $\mathbf{e}_R(\Theta = 0, \Phi) = \mathbf{e}_r(\theta = 0, \varphi) = \mathbf{e}_3$. Inclusion and matrix domains are represented by

$$\begin{aligned} &\Omega = \{(R, \Theta, \Phi) \,|\, R \in (0, R_0), \Theta \in (0, \pi), \Phi \in (0, 2\pi)\}, \\ &B - \Omega = \{(R, \Theta, \Phi) \,|\, R \in (R_0, R_1), \Theta \in (0, \pi), \Phi \in (0, 2\pi)\}. \end{aligned} \tag{1}$$

Spherically symmetric deformations are of the form

$$r = f(R), \quad \theta = \Theta, \quad \varphi = \Phi \tag{2}$$

with principal stretches $\lambda_R = |\mathbf{U}\mathbf{e}_R|$, $\lambda_\Theta = |\mathbf{U}\mathbf{e}_\Theta|$, $\lambda_\Phi = |\mathbf{U}\mathbf{e}_\Phi|$ given by

$$\lambda_R = \lambda^{-2} = f'(R) = (R/r)^2, \quad \lambda_\Theta = \lambda = R^{-1} f(R) = R^{-1} r, \quad \lambda_\Phi = \lambda = R^{-1} f(R) = R^{-1} r, \tag{3}$$

where $\mathbf{U}$ $(= \sqrt{\mathbf{F}^{\mathrm{T}}\mathbf{F}})$ is the right stretch tensor and $\mathbf{F}$ is the deformation gradient associated with (2). In (3) we have used the fact that the incompressibility constraint $\det \mathbf{U} = 1$ may be written in the form

$$R^{-2} f^2 f' = 1. \tag{4}$$

Integration of (4) yields the following expressions for the stretch λ $(= r/R = f(R)/R)$:

$$\lambda = \left[1 + \left(\frac{R_0}{R}\right)^3 (\lambda_0^3 - 1)\right]^{1/3} = \left[1 - \left(\frac{r_0}{r}\right)^3 (1 - \lambda_0^{-3})\right]^{-1/3}, \tag{5}$$

where λ_0 is the interface stretch to be determined. Isotropic, incompressible, hyperelastic matrix material response is characterized, for the deformation (2), by the physical components

$$T_{rr} = \lambda_R \frac{\partial \hat{\sigma}}{\partial \lambda_R} - \hat{\pi}, \quad T_{\theta\theta} = \lambda_\Theta \frac{\partial \hat{\sigma}}{\partial \lambda_\Theta} - \hat{\pi}, \quad T_{\varphi\varphi} = \lambda_\Phi \frac{\partial \hat{\sigma}}{\partial \lambda_\Phi} - \hat{\pi}, \tag{6}$$

where $T_{rr}, T_{\theta\theta}, T_{\varphi\varphi}$ are physical components of the Cauchy stress tensor $\mathbf{T}$, $\hat{\sigma}$ is the strain energy density and $\hat{\pi}$ is hydrostatic pressure. The equilibrium equation $\operatorname{div}\mathbf{T} = \mathbf{0}$ has one non-trivial component which, following Abeyaratne and Horgan (1985), may be written in the form

$$\frac{\partial T_{rr}}{\partial R} + \frac{2f'(R)}{f(R)} T_{rr} - \frac{f'(R)}{f(R)} (T_{\theta\theta} + T_{\varphi\varphi}) = 0, \tag{7}$$

where use has been made of deformation (2). The boundary conditions are a uniform dead load traction and may be written as a condition on the radial component of Cauchy stress by employing the well-known relationship between Piola–Kirchoff stress ($\mathbf{S}$) and Cauchy stress ($\mathbf{S} = (\det \mathbf{F})\mathbf{T}\mathbf{F}^{-\mathrm{T}}$). The result is

$$T_{rr} = \sigma \left(\frac{r_1}{R_1}\right)^{-2} = \sigma \lambda_1^{-2}, \tag{8}$$

where σ is positive and has units of force per unit area in the reference state. The interface boundary condition on the inner surface of the matrix is given by

$$T_{rr} = s_r^0 \quad \text{on } r_0 = f(R_0). \tag{9}$$

The function s_r^0 appearing in (9) is the normal interface traction, which we assume is generally dependent on the ratio of normalized interfacial separation $\lambda_0 - 1$ to a (non-dimensional) characteristic force length parameter ρ. For the case of a non-uniform interface (not considered here), s_r^0 is dependent on the interface coordinates θ, φ as well.

Substituting (4) and (6) into (7) and integrating the result determines the pressure. There are two unknown constants (one is from the integration and the other is λ_0). By employing the boundary conditions (8) and (9) these can be readily determined. The interface equation governing λ_0 is then given by

$$0 = F(\lambda_0,\sigma) = -\sigma + [1 + c(\lambda_0^3 - 1)]^{2/3}\left\{\hat{s}_r^0(\lambda_0) + \int_{[1+c(\lambda_0^3-1)]^{1/3}}^{\lambda_0} \frac{D\hat{w}(\lambda)}{(\lambda^3-1)}\,\mathrm{d}\lambda\right\}, \quad \lambda_0 \geqslant 1, \tag{10}$$

where c is the concentration of inclusion in matrix defined to be $c = (R_0/R_1)^3$ and $\hat{s}_r^0(\lambda_0) = s_r^0((\lambda_0-1)/\rho)$. The stress components $(T_{rr}, T_{\theta\theta}, T_{\varphi\varphi})$ follow from (6) and may be written in the form

$$\begin{aligned} T_{rr} &= \int_{\lambda_1}^{\lambda} \frac{D\hat{w}(t)}{1-t^3}\,\mathrm{d}t + \lambda_1^{-2}\sigma = -\int_{\lambda}^{\lambda_0} \frac{D\hat{w}(t)}{1-t^3}\,\mathrm{d}t + \hat{s}_r^0(\lambda_0), \\ T_{\theta\theta} &= T_{\varphi\varphi} = \frac{1}{2}\lambda D\hat{w}(\lambda) + T_{rr} \end{aligned} \tag{11}$$

with $\hat{w}(\lambda) = \hat{\sigma}(\lambda^{-2},\lambda,\lambda)$. Furthermore, $D\hat{w}(\lambda)$ means $D_\lambda\hat{w}(\lambda)$, i.e., differentiation of the function that follows it with respect to its argument (note that $D_\lambda\hat{w}(\lambda_0)$ indicates differentiation followed by evaluation at λ_0). The pressure function $(\hat{\pi})$ is given by

$$\begin{aligned} \hat{\pi}(\lambda) &= \lambda^{-2}\hat{\sigma}_1(\lambda^{-2},\lambda,\lambda) - \int_{\lambda_1}^{\lambda} \frac{2}{t(1-t^3)}[t\hat{\sigma}_2(t^{-2},t,t) - t^{-2}\hat{\sigma}_1(t^{-2},t,t)]\,\mathrm{d}t - \lambda_1^{-2}\sigma \\ &= \lambda^{-2}\hat{\sigma}_1(\lambda^{-2},\lambda,\lambda) + \int_{\lambda}^{\lambda_0} \frac{2}{t(1-t^2)}[t\hat{\sigma}_2(t^{-2},t,t) - t^{-2}\hat{\sigma}_1(t^{-2},t,t)]\,\mathrm{d}t - \hat{s}_r^0(\lambda_0), \end{aligned} \tag{12}$$

where we have employed the shorthand notation

$$\hat{\sigma}_1(\lambda^{-2},\lambda,\lambda) = \left.\frac{\partial\hat{\sigma}}{\partial\lambda_1}\right|_{\lambda_1=\lambda^{-2}}, \quad \hat{\sigma}_2(\lambda^{-2},\lambda,\lambda) = \hat{\sigma}_3(\lambda^{-2},\lambda,\lambda) = \left.\frac{\partial\hat{\sigma}}{\partial\lambda_2}\right|_{\lambda_1=\lambda}. \tag{13}$$

Note that the stretch at the outer boundary λ_1 $(< \lambda_0)$ follows from (5) provided λ_0 is known.

The potential energy of the sphere Φ consists of the strain energy of the matrix, the interface energy, and the potential energy of the loading applied on the outer surface of the sphere

$$\Phi\{f(R_0)\} = 4\pi\int_{R_0}^{R_1} \hat{\sigma}(f'(R),f(R),f(R))R^2\,\mathrm{d}R + 4\pi\int^{f(R_0)} \hat{s}_r^0(z)z^2\,\mathrm{d}z - 4\pi\sigma[f(R_1) - R_1]R_1^2. \tag{14}$$

Note that in (14) the integral for the interface energy has been computed from the work expression $\int_{t_0}^{t_1}\{\int_{\partial\mathbf{f}(\Omega)} \mathbf{s}_\mathbf{I}(-\mathbf{e}_\mathbf{r})\cdot\mathbf{v}\,\mathrm{d}A\}\,\mathrm{d}t$, where $\mathbf{v}$ is the velocity field and the surface integral is taken over the deformed, inner matrix boundary. The potential energy $\widehat{\boldsymbol{\Phi}}$, normalized with respect to sphere volume $(\frac{4}{3}\pi R_1^3)$, can be written as a function of interface stretch λ_0,

$$c\widehat{\boldsymbol{\Phi}}(\lambda_0) = 3c(\lambda_0^3-1)\int_{[1+c(\lambda_0^3-1)]^{1/3}}^{\lambda_0} \frac{\hat{\sigma}(\lambda^{-2},\lambda,\lambda)\lambda^2}{(\lambda^3-1)^2}\,\mathrm{d}\lambda + 3c\int^{\lambda_0} \hat{s}_r^0(z)z^2\,\mathrm{d}z - 3\sigma\{[1 + c(\lambda_0^3-1)]^{1/3} - 1\}, \tag{15}$$

where use has been made of (3)–(5). Integration by parts applied to the derivative of (15) $D_{\lambda_0}\widehat{\boldsymbol{\Phi}}$, yields the relation $D_{\lambda_0}\widehat{\boldsymbol{\Phi}}(\lambda_0) = 3c\lambda_0^2\lambda_1^{-2}F$, where F is defined in (10) and λ_1 may be written in terms of λ_0 by (5). Thus, equilibrium solutions to interface equation (10) render the potential energy stationary. Conversely, interface stretches λ_0 which make the potential energy stationary are equilibrium solutions to the interface equation. The second derivative of the potential energy is

$$D^2_{\lambda_0}\widehat{\boldsymbol{\Phi}}(\lambda_0) = 2\lambda_0^{-1}D_{\lambda_0}\widehat{\boldsymbol{\Phi}}(\lambda_0) + 3c\lambda_0^2\left[\frac{D_\lambda\hat{w}(\lambda_0)}{\lambda_0^3-1} - \frac{c\lambda_0^2 D_\lambda\hat{w}(\lambda_1)}{\lambda_1^2(\lambda_1^3-1)} + 2c\sigma\frac{\lambda_0^2}{\lambda_1^5} + D_{\lambda_0}\hat{s}_r^0(\lambda_0)\right], \tag{16}$$

and we say that an equilibrium interface stretch λ_0 is infinitesimally superstable [1] or more simply, locally stable when $D^2_{\lambda_0}\widehat{\boldsymbol{\Phi}}(\lambda_0) > 0$, i.e., λ_0 renders the potential energy a local minimum.

2.2. Basic equations for the power law material matrix

In what follows, we assume matrix material response can be modeled by the incompressible constitutive relation

$$\mathbf{S_0} = \frac{2}{3}\frac{S_{\text{eq}}}{E_{\text{eq}}}\mathbf{E}, \tag{17}$$

where $\mathbf{E}$ is the infinitesimal strain tensor, $\mathbf{S_0}$ is the deviatoric stress tensor defined to be $\mathbf{S} - 1/3(\text{tr}\mathbf{S})\mathbf{1}$ with tr$[\cdot]$ indicating trace and $\mathbf{1}$ the unit tensor. The quantities S_{eq} and E_{eq} are the equivalent stress and strain, respectively, and are defined by

$$E_{\text{eq}} = \sqrt{\frac{2}{3}\mathbf{E}\cdot\mathbf{E}}, \quad S_{\text{eq}} = \sqrt{\frac{3}{2}\mathbf{S_0}\cdot\mathbf{S_0}}. \tag{18}$$

S_{eq} and E_{eq} are such that for uniaxial stress σ, $S_{\text{eq}} = \sigma$ and $E_{\text{eq}} = \varepsilon$, the axial strain. The constitutive relation (17) must be supplemented by a relationship between S_{eq} and E_{eq}. In this paper, we assume that uniaxial behavior is accurately represented by the piecewise smooth, power law relation so that S_{eq} and E_{eq} are related by

$$S_{\text{eq}} = \begin{cases} \dfrac{\sigma_y}{\varepsilon_y}E_{\text{eq}}, & E_{\text{eq}} \leqslant \varepsilon_y, \\ \sigma_y\left(\dfrac{E_{\text{eq}}}{\varepsilon_y}\right)^N, & E_{\text{eq}} \geqslant \varepsilon_y, \end{cases} \tag{19}$$

where $N \in [0,1]$ is the strain hardening exponent, σ_y is the yield stress, ε_y is the (infinitesimal) yield strain and the ratio σ_y/ε_y is the elastic modulus E. The energy density function $\hat{w}$ defined by $\hat{w}(\lambda) = \hat{\sigma}(\lambda^{-2},\lambda,\lambda)$ and associated with (17) and (19) is given by

$$\hat{w}(\lambda) = \begin{cases} \dfrac{1}{2}\dfrac{\sigma_y}{\varepsilon_y}E^2_{\text{eq}}(\lambda), & E_{\text{eq}}(\lambda) \leqslant \varepsilon_y, \\ \dfrac{N-1}{2(N+1)}\sigma_y\varepsilon_y + \dfrac{\sigma_y\varepsilon_y}{N+1}\left(\dfrac{E_{\text{eq}}(\lambda)}{\varepsilon_y}\right)^{N+1}, & E_{\text{eq}}(\lambda) \geqslant \varepsilon_y, \end{cases} \tag{20}$$

where the functional dependence of E_{eq} on the stretch λ needs to be specified for a given deformation. The derivative $\text{D}\hat{w}(\lambda)$ follows from (20) and is

$$\text{D}\hat{w}(\lambda) = S_{\text{eq}}(\lambda)\text{D}E_{\text{eq}}(\lambda) = \begin{cases} \sigma_y\dfrac{E_{\text{eq}}(\lambda)}{\varepsilon_y}\text{D}E_{\text{eq}}(\lambda), & E_{\text{eq}}(\lambda) \leqslant \varepsilon_y, \\ \sigma_y\left(\dfrac{E_{\text{eq}}(\lambda)}{\varepsilon_y}\right)^N\text{D}E_{\text{eq}}(\lambda), & E_{\text{eq}}(\lambda) \geqslant \varepsilon_y. \end{cases} \tag{21}$$

[1] In the sense of Truesdell and Noll (1965).

Now recall the principal stretches (3). Then the infinitesimal radial strain E_{rr} and the infinitesimal circumferential strain $\varepsilon = E_{\theta\theta} = E_{\varphi\varphi}$ are given by

$$\begin{aligned} &E_{rr} = \lambda_R - 1 = \lambda^{-2} - 1 = -2(\lambda - 1) + \mathrm{O}(\lambda - 1)^2, \\ &\varepsilon = E_{\theta\theta} = E_{\Phi\Phi} = \lambda_\Theta - 1 = \lambda - 1. \end{aligned} \tag{22}$$

Note that the constraint of incompressibility in infinitesimal deformation is satisfied since, to a term of order $\mathrm{O}(\lambda - 1)^2$, $\mathrm{tr}\,\mathbf{E} = 0$ as required. By combining (18) and (22) we get

$$E_{\mathrm{eq}}(\lambda) = 2(\lambda - 1), \quad \mathrm{D}E_{\mathrm{eq}}(\lambda) = 2, \tag{23}$$

so that the energy density function (21) is completely specified as a function of stretch λ or circumferential strain ε $(= \lambda - 1)$.

Before Eqs. (10)–(12) can be written in terms of strain energy density gradient (21) and (23) we need to linearize them in an appropriate way so that we maintain non-linear material response at infinitesimal strain. We can do this because $\mathrm{D}\hat{w}(\lambda)$ is actually a function of the ratio $(\lambda - 1)/\varepsilon_y$ which remains finite for stretches λ near unity. Consider the integral

$$\int_{[[1+c((\varepsilon_y\Gamma_0+1)^3-1)]^{1/3}-1]/\varepsilon_y}^{\Gamma_0} \frac{\varepsilon_y \mathrm{D}\hat{w}(\Gamma)}{\left((\varepsilon_y\Gamma + 1)^3 - 1\right)}\,\mathrm{d}\Gamma,$$

which is obtained from the integral in (10) with the substitution $\Gamma = (\lambda - 1)/\varepsilon_y$. Now expand the integral in a series in ε_y keeping Γ, Γ_0 finite. Neglecting terms of order $\mathrm{O}(\varepsilon_y)$ results in the approximation

$$\frac{1}{3}\int_{c\Gamma_0}^{\Gamma_0} \frac{\mathrm{D}\hat{w}(\Gamma)}{\Gamma}\,\mathrm{d}\Gamma.$$

A similar result is stated in Chung et al. (1987) in the context of cavity nucleation in a solid sphere. Using (21)–(23), (10) governing the interface stretch may now be written in the infinitesimal strain form

$$0 = F(\varepsilon_0, \sigma) = -\sigma + s_r^0\left(\frac{\varepsilon_0}{\rho}\right) + \frac{2}{3}\int_{c\varepsilon_0/\varepsilon_y}^{\varepsilon_0/\varepsilon_y} \frac{S_{\mathrm{eq}}(\Gamma)}{\Gamma}\,\mathrm{d}\Gamma, \tag{24}$$

where ε_0 $(= \lambda_0 - 1)$ measures both the circumferential strain at the interface and the radial interface displacement discontinuity. Note that we will assume that parameter ρ is such that the ratio ε_0/ρ remains finite in the limit of infinitesimal ε_0. By substituting (19) and (23) into (24) we get the infinitesimal strain version of the interface equation for the power law material matrix

$$\sigma = \begin{cases} s_r^0\left(\dfrac{\varepsilon_0}{\rho}\right) + \dfrac{4}{3}(1-c)E\varepsilon_0, & \dfrac{2\varepsilon_0}{\varepsilon_y} \leqslant 1, \\ s_r^0\left(\dfrac{\varepsilon_0}{\rho}\right) + \dfrac{2}{3}\sigma_y\left\{\dfrac{1}{N}\left[\left(\dfrac{2\varepsilon_0}{\varepsilon_y}\right)^N - 1\right] + 1 - c\dfrac{2\varepsilon_0}{\varepsilon_y}\right\}, & \dfrac{2c\varepsilon_0}{\varepsilon_y} \leqslant 1 \leqslant \dfrac{2\varepsilon_0}{\varepsilon_y}, \\ s_r^0\left(\dfrac{\varepsilon_0}{\rho}\right) + \dfrac{2}{3}\dfrac{\sigma_y}{N}(1-c^N)\left(\dfrac{2\varepsilon_0}{\varepsilon_y}\right)^N, & 1 \leqslant \dfrac{2c\varepsilon_0}{\varepsilon_y} \leqslant \dfrac{2\varepsilon_0}{\varepsilon_y}. \end{cases} \tag{25}$$

The different functional forms of the equation depend upon whether the matrix shell is fully elastic $2\varepsilon_0 \leqslant \varepsilon_y$, elasto-plastic $2c\varepsilon_0 \leqslant \varepsilon_y \leqslant 2\varepsilon_0$ or fully plastic $\varepsilon_y \leqslant 2c\varepsilon_0 \leqslant 2\varepsilon_0$ (note that the quantity $c\varepsilon_0$ is the circumferential strain at the outer boundary of the composite sphere). For the case of the non-hardening matrix, take the limit of (25) as $N \downarrow 0$ to get

$$\sigma = \begin{cases} s_r^0\left(\dfrac{\varepsilon_0}{\rho}\right) + \dfrac{4}{3}(1-c)E\varepsilon_0, & \dfrac{2\varepsilon_0}{\varepsilon_y} \leqslant 1, \\ s_r^0\left(\dfrac{\varepsilon_0}{\rho}\right) + \dfrac{2}{3}\sigma_y\left[\log\left(\dfrac{2\varepsilon_0}{\varepsilon_y}\right) + 1 - c\dfrac{2\varepsilon_0}{\varepsilon_y}\right], & \dfrac{2c\varepsilon_0}{\varepsilon_y} \leqslant 1 \leqslant \dfrac{2\varepsilon_0}{\varepsilon_y}, \\ s_r^0\left(\dfrac{\varepsilon_0}{\rho}\right) + \dfrac{2}{3}\sigma_y \log c^{-1}, & 1 \leqslant \dfrac{2c\varepsilon_0}{\varepsilon_y} \leqslant \dfrac{2\varepsilon_0}{\varepsilon_y}. \end{cases} \tag{26}$$

The spherical components of stress field **(S)** for infinitesimal strains follow from (11), (21) and (23) by a similar limit process used to obtain (24). The result is

$$\begin{aligned} S_{rr} &= s_r^0\left(\frac{\varepsilon_0}{\rho}\right) - \frac{2}{3}\int_{\varepsilon_0/\varepsilon_y}^{\varepsilon/\varepsilon_y} \frac{S_{\mathrm{eq}}(\Gamma)}{\Gamma}\,\mathrm{d}\Gamma, \\ S_{\theta\theta} &= S_{\varphi\varphi} = S_{rr} + S_{\mathrm{eq}}\left(\frac{\varepsilon}{\varepsilon_y}\right), \end{aligned} \tag{27}$$

where S_{eq} is given by (19) and we note from (5) that, to a term of order $\mathrm{O}(\lambda_0 - 1)^2$,

$$\varepsilon = \lambda - 1 = \left(\frac{R_0}{R}\right)^3 \varepsilon_0. \tag{28}$$

2.3. Spherically symmetric bifurcation; stability of equilibria

Eqs. (25)–(27) may be used to predict spherically symmetric behavior under increasing load σ. First, the critical load required to initiate plasticity at the inner matrix boundary follows from $(25)_1$ for the power law matrix and from $(26)_1$ for the non-hardening matrix provided $\varepsilon_0 = \varepsilon_y/2$,

$$\sigma = s_r^0\left(\frac{\sigma_y}{2E\rho}\right) + \frac{2}{3}(1-c)\sigma_y. \tag{29}$$

Note that we are assuming bifurcation of interface separation occurs at a load σ greater than that required to initiate plasticity at the inner matrix surface. The simpler case of bifurcation in an elastic matrix follows by simply letting $N = 1$ in the following results. Implicit in (29) are the two limiting cases of void behavior $(s_r^0(\cdot) = 0)$ in which the critical load increases linearly with yield stress, and rigid interface behavior in which no amount of load is adequate to initiate yield at the interface.

Bifurcation of equilibrium interfacial separation is governed by $F(\varepsilon_0, \sigma) = \mathrm{D}_{\varepsilon_0} F(\varepsilon_0, \sigma) = 0$ where the function F is defined by (25) (or (26)). The solutions of these equations, when they exist, generate bifurcation points $(\sigma^*, \varepsilon_0^*)$. A Taylor series of F about a given bifurcation point is then usually adequate to obtain the local behavior of the solutions near the point in question. These calculations will not be carried out here since they yield no information that is not obtainable from a direct numerical determination of the equilibria governed by (25) or (26). It is of interest though to examine the bifurcation condition $\mathrm{D}_{\varepsilon_0} F(\varepsilon_0, \sigma) = 0$. For the power law matrix,

$$0 = \rho \mathrm{D}_{\varepsilon_0} F = \begin{cases} \mathrm{D}_{\varepsilon_0/\rho} s_r^0\left(\dfrac{\varepsilon_0}{\rho}\right) + \dfrac{4}{3}(1-c)\rho E, & \dfrac{2\varepsilon_0}{\varepsilon_y} \leqslant 1, \\ \mathrm{D}_{\varepsilon_0/\rho} s_r^0\left(\dfrac{\varepsilon_0}{\rho}\right) + \dfrac{2}{3}\dfrac{\rho\sigma_y}{\varepsilon_0}\left\{\left(\dfrac{2\varepsilon_0}{\varepsilon_y}\right)^N - \dfrac{2c\varepsilon_0}{\varepsilon_y}\right\}, & \dfrac{2c\varepsilon_0}{\varepsilon_y} \leqslant 1 \leqslant \dfrac{2\varepsilon_0}{\varepsilon_y}, \\ \mathrm{D}_{\varepsilon_0/\rho} s_r^0\left(\dfrac{\varepsilon_0}{\rho}\right) + \dfrac{2}{3}\dfrac{\rho\sigma_y}{\varepsilon_0}(1-c^N)\left(\dfrac{2\varepsilon_0}{\varepsilon_y}\right)^N, & 1 \leqslant \dfrac{2c\varepsilon_0}{\varepsilon_y} \leqslant \dfrac{2\varepsilon_0}{\varepsilon_y}, \end{cases} \tag{30}$$

while for the non-hardening matrix,

$$= \rho \mathrm{D}_{\varepsilon_0} F = \begin{cases} \mathrm{D}_{\varepsilon_0/\rho} s_r^0\left(\dfrac{\varepsilon_0}{\rho}\right) + \dfrac{4}{3}(1-c)\rho E, & \dfrac{2\varepsilon_0}{\varepsilon_y} \leqslant 1, \\ \mathrm{D}_{\varepsilon_0/\rho} s_r^0\left(\dfrac{\varepsilon_0}{\rho}\right) + \dfrac{2}{3}\dfrac{\rho\sigma_y}{\varepsilon_0}\left\{1 - \dfrac{2c\varepsilon_0}{\varepsilon_y}\right\}, & \dfrac{2c\varepsilon_0}{\varepsilon_y} \leqslant 1 \leqslant \dfrac{2\varepsilon_0}{\varepsilon_y}, \\ \mathrm{D}_{\varepsilon_0/\rho} s_r^0\left(\dfrac{\varepsilon_0}{\rho}\right), & 1 \leqslant \dfrac{2c\varepsilon_0}{\varepsilon_y} \leqslant \dfrac{2\varepsilon_0}{\varepsilon_y}. \end{cases} \tag{31}$$

Thus, spherically symmetric bifurcation occurs when $\mathrm{D}_{\varepsilon_0/\rho} s_r^0(\varepsilon_0/\rho) \leqslant 0$ where the equality applies when the spherical shell is fully plastic and non-hardening $(31)_3$ and the inequality applies in all other cases, i.e., when the interfacial separation is on the descending branch of the interface force-separation curve. Now consider bifurcation condition $(30)_2$ governing the partially plastic matrix shell

$$\frac{\sigma_{\max}}{\sigma_y}\mathrm{D}_{\Gamma_0} s(\Gamma_0) + \frac{2}{3}\frac{1}{\Gamma_0}\left\{\left(2\frac{\rho}{\varepsilon_y}\Gamma_0\right)^N - 2c\frac{\rho}{\varepsilon_y}\Gamma_0\right\} = 0, \tag{32}$$

where Γ_0 is ε_0/ρ and $s = s_r^0/\sigma_{\max}$, $\sigma_{\max}$ (the interface strength) being a characteristic of the interface force law. Whether or not solutions to (32) exist determines the spherically symmetric bifurcation characteristics for a particular system, i.e., the linear elastic matrix shell $(N = 1, c \in (0,1))$, the power law matrix shell $(N \in (0,1), c \in (0,1))$, the non-hardening matrix shell $(N = 0, c \in (0,1))$ and the unbounded matrix $(c = 0)$. The existence of solutions to (32) will generally depend on c, N and the ratios $\sigma_{\max}/\sigma_y$, ρ/ε_y. For the special case of an unbounded non-hardening matrix $(N = 0, c = 0)$, (32) becomes independent of the ratio ρ/ε_y so that the interface force length parameter (ρ) cannot influence whether or not bifurcation will occur. More specifically, consider the simple physically based exponential interface force law of Ferrante et al. (1982)

$$s_r^0\left(\frac{\lambda_0 - 1}{\rho}\right) = e\sigma_{\max}\frac{\lambda_0 - 1}{\rho}\mathrm{e}^{-(\lambda_0 - 1)/\rho}, \tag{33}$$

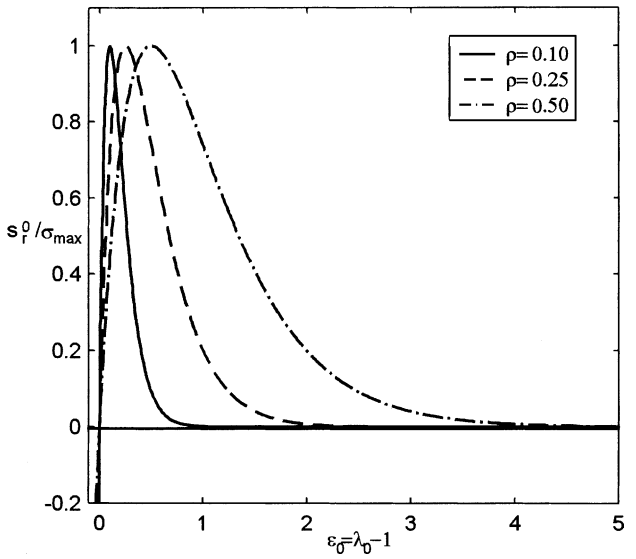

Fig. 1. The interface force law.

where $\sigma_{\max}$ is the interface strength, and dimensionless force length parameter ρ characterizes the range of action of the force law (Fig. 1). For the linear elastic matrix ($N = 1$) (32) and (33) imply that

$$\frac{\varepsilon_0^*}{\rho} = 1 - W\left(-\frac{4}{3}(1-c)\frac{\rho/\varepsilon_y}{\sigma_{\max}/\sigma_y} \right), \tag{34}$$

where W is the multi-valued Lambert W function defined to be the solution y to the equation $ye^y = x$ (Corless et al., 1993). Since W is defined on the domain $[-e^{-1}, \infty)$, we require that

$$\frac{4}{3}(1-c)\frac{\rho/\varepsilon_y}{\sigma_{\max}/\sigma_y} \in [0, e^{-1}]$$

be satisfied for the existence of bifurcation points which occur in pairs (an entirely analogous situation has been shown to exist in a planar setting (Levy, 1998)). Note that the critical load at bifurcation follows by substituting (34) in $(25)_1$. Simple solutions to (32) and (33) do not exist for $N \in [0, 1)$. However, for the unbounded ($c = 0$) non-hardening matrix ($N = 0$) insight into the bifurcation behavior can be obtained by noting that for this case (32) and (33) imply that

$$\frac{\varepsilon_0^*}{\rho} = f\left(\frac{\sigma_{\max}}{\sigma_y} \right), \tag{35}$$

where f is the function shown in Fig. 2. The figure indicates that for $\sigma_{\max}/\sigma_y \in [0, 0.794)$ no solutions to (32) and (33) exist so there are no spherically symmetric bifurcations when the matrix shell is partially plastic. For values $\sigma_{\max}/\sigma_y \in [0.794, \infty)$ there are two solutions to (32) and (33) and therefore two bifurcation points. Furthermore, as stated previously, only for this case does the force length parameter ρ not affect the character of solutions or, the existence of spherically symmetric bifurcations. Another aspect of behavior is whether spherically symmetric equilibrium solutions exist for the partially plastic, or fully plastic matrix shell in the post bifurcation regime. This aspect of behavior, as well as others, will be explored below.

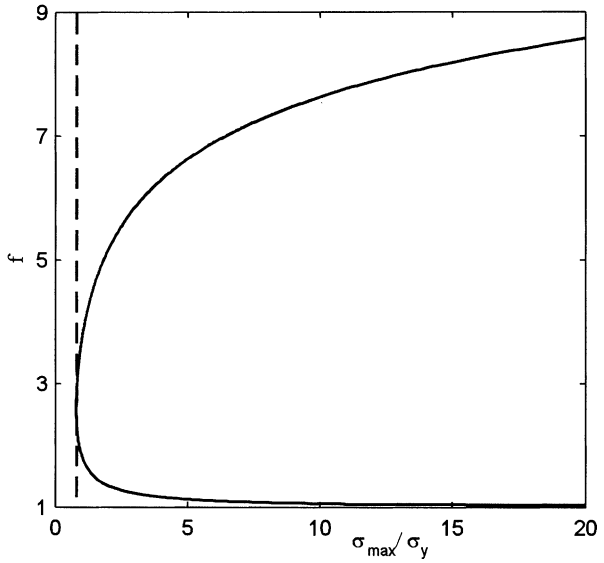

Fig. 2. The function $f(\sigma_{\max}/\sigma_y)$.

An analysis of stability can proceed once the potential energy is written for the infinitesimally deformed power law matrix sphere. Introduce the quantity $\Gamma = (\lambda - 1)/\varepsilon_y = \varepsilon/\varepsilon_y$ in (15) and expand the result in a series in ε_y retaining only linear terms. The result is

$$\widehat{\Phi}(\varepsilon_0) = c\frac{\varepsilon_0}{\varepsilon_y}\int_{c\varepsilon_0/\varepsilon_y}^{\varepsilon_0/\varepsilon_y}\frac{\hat{w}(\Gamma)}{\Gamma^2}\,\mathrm{d}\Gamma + 3c\varepsilon_y\int^{\varepsilon_0/\varepsilon_y} s_r^0\left(\Gamma\frac{\varepsilon_y}{\rho}\right)\mathrm{d}\Gamma - 3\sigma c\varepsilon_0, \tag{36}$$

where $\hat{w}$ is given by (20) and where we have assumed that both Γ and the ratio ε_y/ρ are finite. It follows directly from (36) that

$$\mathrm{D}_{\varepsilon_0}\widehat{\Phi} = 3cF, \quad \mathrm{D}^2_{\varepsilon_0}\widehat{\Phi} = 3c\mathrm{D}_{\varepsilon_0}F, \tag{37}$$

where F is given by (24), and where $\rho\mathrm{D}_{\varepsilon_0}F$ for the hardening matrix is given by (30) and for the non-hardening matrix by (31). Below we consider the two limiting cases of the elastic matrix ($N = 1$) and the non-hardening matrix ($N = 0$). We assume that the interface law is of the form (33) or, has the properties: $s_r^0(0) = 0$, $\mathrm{D}s_r^0(\varepsilon_0/\rho)$ has a single maximum on $\varepsilon_0/\rho \in [0,\infty)$, $s_r^0(\varepsilon_0/\rho) = \mathrm{D}s_r^0(\varepsilon_0/\rho) = 0$, $\varepsilon_0/\rho \uparrow \infty$ and $\mathrm{D}^2 s_r^0(\varepsilon_0/\rho)$ vanishes at two points one of which is at infinity.

The elastic case ($N = 1$). It follows from (30), $(37)_2$ and the local stability definition that, for $N = 1$, equilibrium states are locally stable provided, $\mathrm{D}s_r^0(\varepsilon_0/\rho) > -\frac{4}{3}(1-c)\rho E$. Note that, except for the case where the line $-\frac{4}{3}(1-c)\rho E$ is tangent to the curve $\mathrm{D}s_r^0(\varepsilon_0/\rho)$, there are two (bifurcation) points that satisfy $\mathrm{D}s_r^0(\varepsilon_0/\rho) = -\frac{4}{3}(1-c)\rho E$ if there is one point that satisfies it (this has been stated another way in the discussion following (34)). These points bound the branch of unstable equilibrium states (Fig. 3). Note that the slope $\mathrm{D}s_r^0(\varepsilon_0/\rho)$ can be negative at stable equilibrium states. If $\mathrm{D}s_r^0(\varepsilon_0/\rho) > -\frac{4}{3}(1-c)\rho E$ for all values of ε_0/ρ then the curves never intersect, there are no bifurcation points and all equilibrium states are stable. The existence of a pair of distinct bifurcation points is therefore necessary and sufficient for the existence of unstable equilibrium states.

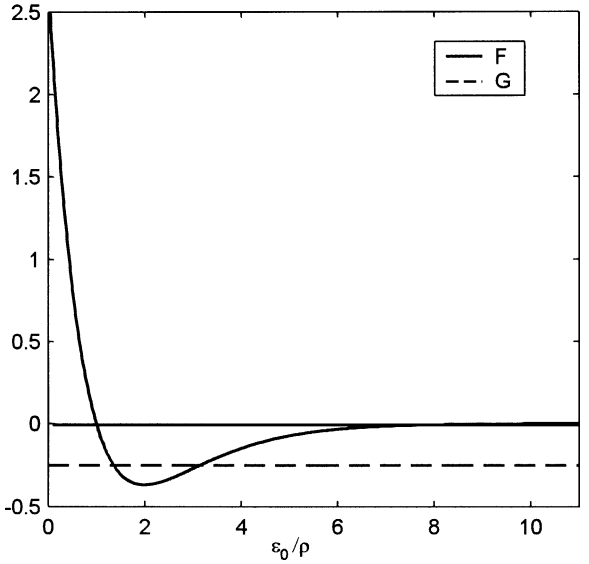

Fig. 3. Stability behavior. Elastic matrix. $F = \mathrm{D}s_r^0(\varepsilon_0/\rho)$, $G = -4(1-c)\rho E/3$. $c = 0.05$, $\rho/\varepsilon_y = 1$, $\sigma_{\max}/\sigma_y = 5$.

The non-hardening case ($N = 0$). For this case (31) indicates that equilibrium states are locally stable if

$$\mathrm{D}s_r^0\left(\frac{\varepsilon_0}{\rho}\right) > \begin{cases} -\dfrac{4}{3}(1-c)\rho E, & \dfrac{2\varepsilon_0}{\varepsilon_y} \leqslant 1, \\ -\dfrac{2}{3}\sigma_y\left\{\dfrac{1}{\varepsilon_0/\rho} - \dfrac{2c\rho}{\varepsilon_y}\right\}, & \dfrac{2c\varepsilon_0}{\varepsilon_y} \leqslant 1 \leqslant \dfrac{2\varepsilon_0}{\varepsilon_y}, \\ 0, & 1 \leqslant \dfrac{2c\varepsilon_0}{\varepsilon_y} \leqslant \dfrac{2\varepsilon_0}{\varepsilon_y}, \end{cases} \tag{38}$$

where $(38)_1$ applies when the matrix shell is elastic, $(38)_2$ applies when the shell is elastic–plastic, and $(38)_3$ applies when the shell is fully plastic. Assume that the first bifurcation point occurs when the matrix is elastic–plastic or fully plastic. Two of the three possible cases are presented as plots of the left-hand side of (38) and the right-hand side of (38). In Fig. 4a, there are three bifurcation points and four distinct stability regions. The origin and the first bifurcation point bound a region of stable behavior. The first two bifurcation points bound a region of unstable behavior. The third bifurcation point (not visible in Fig. 4a) arises from the fact that $\mathrm{D}s_r^0(\varepsilon_0/\rho)$ vanishes from below as its argument approaches infinity (and therefore must intersect the right-hand side of $(38)_2$ before $\varepsilon_0/\rho = \varepsilon_y/(2c\rho)$). Thus, the second and third bifurcation points bound a region of stable states but equilibria lying to the right of the third bifurcation point are unstable. This must occur prior to the state when the matrix becomes fully plastic. (Note that the matrix becomes fully plastic when $\varepsilon_0/\rho = \varepsilon_y/(2c\rho)$, which for the data of Fig. 4 is $\varepsilon_0/\rho = 10$.) The next case (Fig. 4b) shows that there is one bifurcation point that divides the response into stable states (to the left of the bifurcation point) and unstable states (to the right). The third possibility (not shown) is such that $\mathrm{D}s_r^0(\varepsilon_0/\rho)$ remains positive throughout the elastic–plastic response of the matrix shell. When the matrix is fully plastic, bifurcation will occur when the slope $\mathrm{D}s_r^0(\varepsilon_0/\rho)$ vanishes. Thus, it is possible to have stable equilibrium states when the sphere is fully plastic but the sphere will lose stability when the interface force law attains its maximum value. In contrast to the elastic case bifurcation will ultimately always occur.

The case of the hardening matrix will not be given separate treatment. It is similar to the elastic matrix because the term

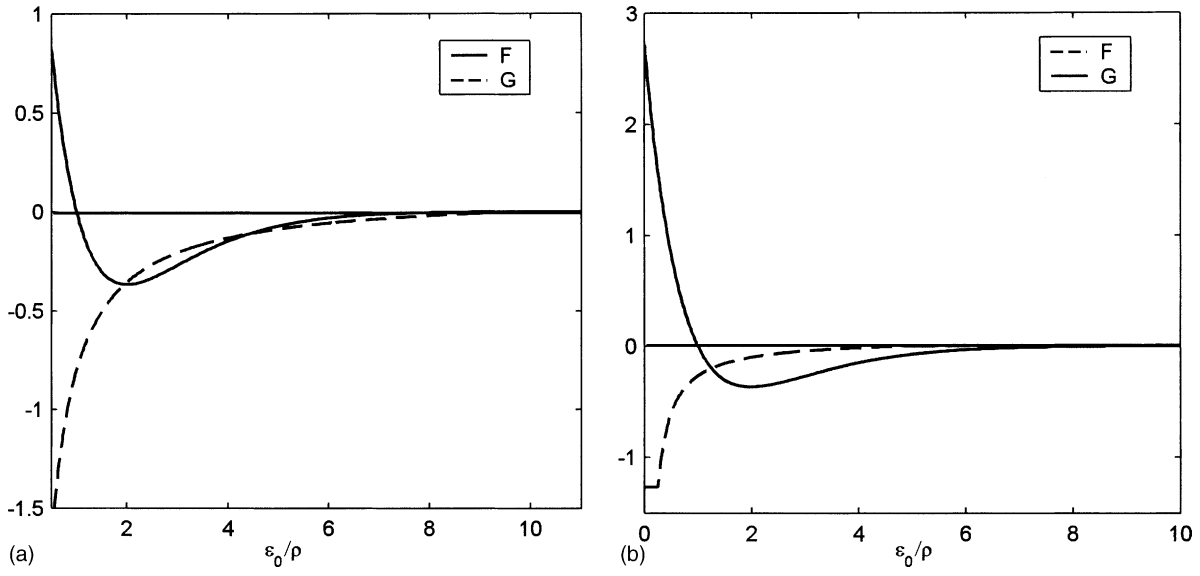

Fig. 4. Stability behavior. Non-hardening matrix. $F = \mathrm{D}s_r^0(\varepsilon_0/\rho)$, $G =$ RHS of (38). (a) $c = 0.05$, $\rho/\varepsilon_y = 1$, $\sigma_{\max}/\sigma_y = 3/4$; (b) $c = 0.05$, $\rho/\varepsilon_y = 2$, $\sigma_{\max}/\sigma_y = 2$.

$$-\frac{2}{3}\frac{\rho\sigma_y}{\varepsilon_0}(1-c^N)\left(\frac{2\varepsilon_0}{\varepsilon_y}\right)^N$$

in $(30)_3$ vanishes from below (more slowly than $\mathrm{D}s_r^0(\varepsilon_0/\rho)$) as its argument $\varepsilon_0/\varepsilon_y$ approaches infinity.

Figs. 5 and 6 are obtained from (25) and (26) and depict graphs of normalized boundary traction (σ/σ_y) versus normalized interface separation (strain) $\varepsilon_0/\varepsilon_y$ for various values of parameters. The data used in the

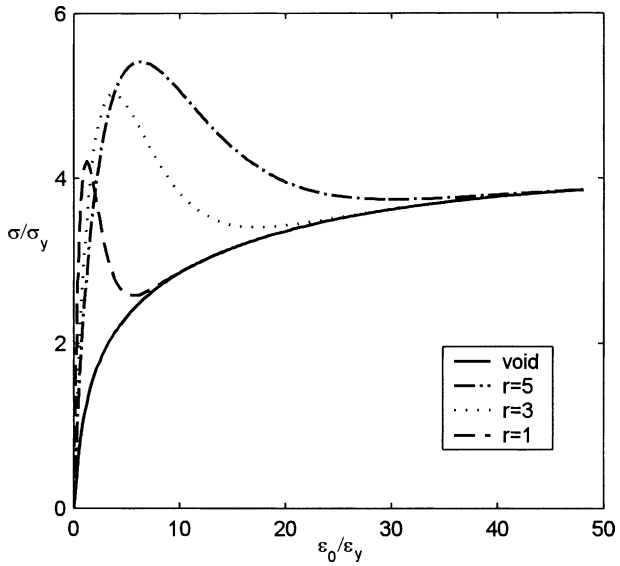

Fig. 5. Load versus strain. $r=\rho/\varepsilon_y$, $\sigma_{\max}=3\sigma_y$, $\sigma_y=0.002\mathrm{E}$, $c=0.0104$, $N=0.1$.

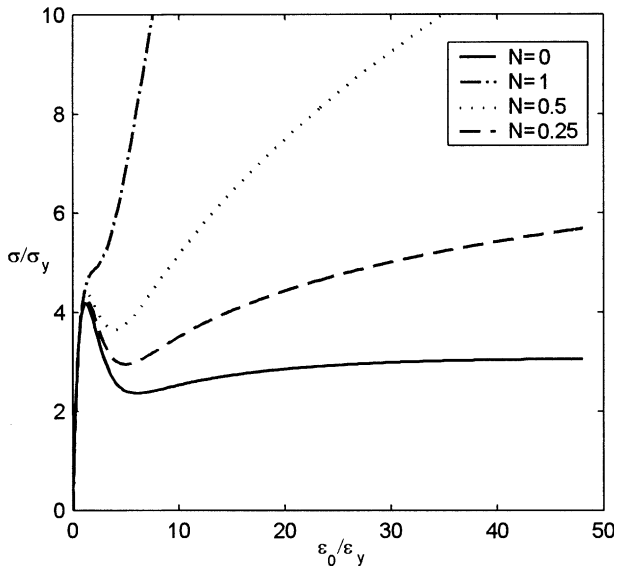

Fig. 6. Load versus strain. $r=\rho/\varepsilon_y=1$, $\sigma_{\max}=3\sigma_y$, $\sigma_y=0.002\mathrm{E}$, $c=0.0104$.

calculations is taken from Needleman (1987) and corresponds to spheroidized steel ($\sigma_y = 0.002E$, $\sigma_{\max} = 3\sigma_y$, $c = 0.0104$). Fig. 5 shows the effect of normalized force length parameter ρ/ε_y on response for a hardening coefficient $N = 0.1$. The domain depicted in the figure is $\varepsilon_0/\varepsilon_y \in (0, (2c)^{-1})$ where the upper bound is that point where the sphere becomes fully plastic. Clearly increasing the force length parameter raises the critical load at bifurcation. Note that all curves are bounded by the rigidly bonded interface solution ($\varepsilon_0/\varepsilon_y = 0$) and by the void solution, which is approached asymptotically as indicated in the figure. Fig. 6 depicts the response for various values of strain hardening exponent N assuming a force length ratio $\rho/\varepsilon_y = 1$. All curves are bounded by linear elastic response ($N = 1$) and perfectly plastic response ($N = 0$). The effect of decreasing the strain-hardening exponent is to decrease the critical load at bifurcation. Furthermore, there are two threshold values of N obtainable from (25) and (30). For values of N greater then 0.874 no bifurcation occurs and the response is the gradual separation of the interface. For N less then 0.874 but greater then 0.148 bifurcation occurs characterized by the abrupt transition between two equilibrium interface separation states. For values of N less then 0.148 there are no spherically symmetric equilibrium solutions after bifurcation which signals the transition to non-symmetric equilibrium states or, dynamic response. Note that the lack of spherically symmetric equilibria in the post bifurcation regime can occur when there are two bifurcation points (Fig. 6, $N = 0$ curve) or, when there is one bifurcation point, i.e., the curve monotonically decreases from its maximum and approaches a local minimum at infinity (recall Fig. 4b). Finally, note that Figs. 5 and 6 are essentially plots of applied boundary traction versus circumferential boundary strain (recall that the circumferential boundary strain is $c\varepsilon_0$).

The evolution of the elasto-plastic boundary may be obtained as follows. Assume that (29) is satisfied and that the boundary between elastic response and power law response is located at a radius R_* with $R_* \in (R_0, R_1)$. Then $\varepsilon_* = \varepsilon_y/2$ so that, by $(25)_2$ (or $(26)_2$) and (28) we have

$$\sigma = \begin{cases} s_r^0\left(\dfrac{\varepsilon_y}{2\rho}\left(\dfrac{R_*}{R_0}\right)^3\right) + \dfrac{2}{3}\sigma_y\left\{\dfrac{1}{N}\left[\left(\dfrac{R_*}{R_0}\right)^{3N} - 1\right] + 1 - c\left(\dfrac{R_*}{R_0}\right)^3\right\}, & N > 0, \\ s_r^0\left(\dfrac{\varepsilon_y}{2\rho}\left(\dfrac{R_*}{R_0}\right)^3\right) + \dfrac{2}{3}\sigma_y\left\{\log\left(\dfrac{R_*}{R_0}\right)^3 + 1 - c\left(\dfrac{R_*}{R_0}\right)^3\right\}, & N = 0, \end{cases} \tag{39}$$

which are algebraic equations governing the evolution of R_*/R_0 with σ, for the hardening and non-hardening matrix, respectively. They may be readily solved once an interface force-separation relation $s_r^0(\varepsilon_0/\rho)$ has been prescribed. Figs. 7 and 8 are graphs of (39) for the interface force law (33). Note that in both figures the range of R_*/R_0 is $(1, c^{-1/3})$, i.e., the elasto-plastic boundary lies between the inner and outer radius of the matrix shell. Fig. 7 shows response for various values of normalized force length parameter ρ/ε_y and for a hardening coefficient $N = 0.1$. (All other parameter values are the same as in Figs. 5 and 6.) For the void, the elasto-plastic boundary evolves continuously with increasing boundary traction σ and this curve is approached by all of the others as the interface separates. The remaining curves indicate a discontinuous change in elasto-plastic boundary under increasing load. This phenomenon coincides with the rapid unloading of the interface and the abrupt increase in the radius of the inner matrix boundary. The response after this transition corresponds to a material still deforming according to the non-linear power law. In an actual metallic material, this would not be the case since linear elastic unloading of matrix material would accompany the sudden reduction in interface traction. Furthermore, with decreasing ratio ρ/ε_y this transition occurs sooner although the initial yield at the inner matrix boundary is delayed. Fig. 8 shows the dependence of elasto-plastic boundary evolution on strain hardening coefficient. Clearly, the effect of straining hardening is to tend to reduce the destabilizing effects of abrupt unloading of the interface as noted previously.

The radial stress component in the elastic zone $R \in (R_*, R_1)$ of the partially plastic matrix, with elasto-plastic boundary at R_*, is obtained from $(27)_1$, (19) and (23) provided we recall (28) and note that $\varepsilon_* = \varepsilon_y/2$,

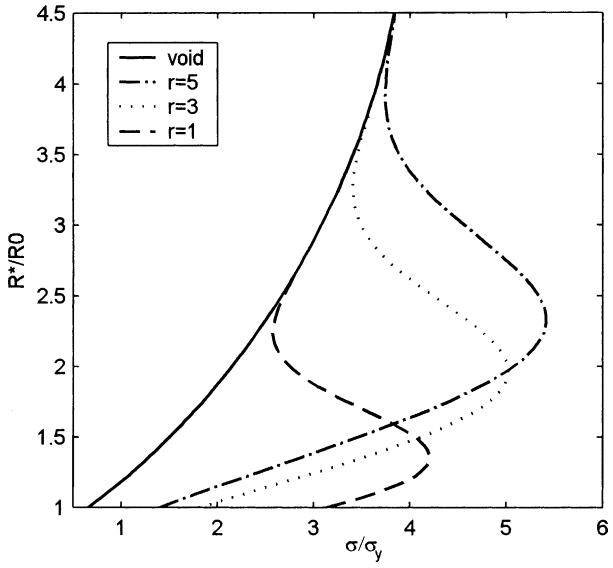

Fig. 7. Elasto-plastic boundary radius versus load. $r = \rho/\varepsilon_y$ (Data as in Fig. 5.)

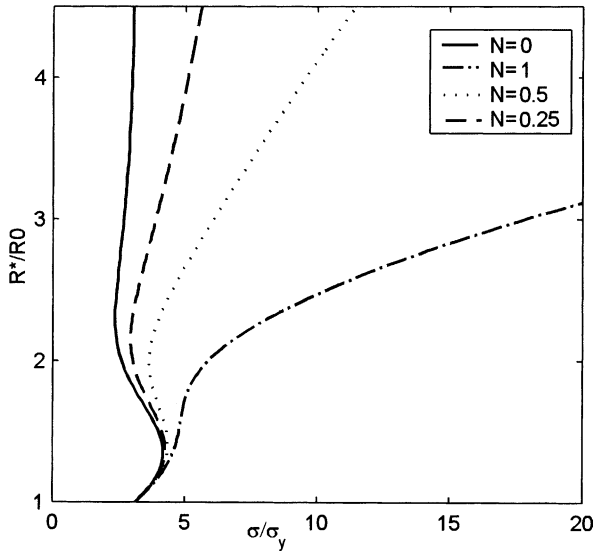

Fig. 8. Elasto-plastic boundary radius versus load. (Data as in Fig. 6.)

$$S_{rr}(R,R_*) = \begin{cases} s_r^0\left(\dfrac{\varepsilon_y}{2\rho}\left(\dfrac{R_*}{R_0}\right)^3\right) + \dfrac{2}{3}\sigma_y\left\{\dfrac{1}{N}\left[\left(\dfrac{R_*}{R_0}\right)^{3N} - 1\right] + 1 - \left(\dfrac{R_*}{R}\right)^3\right\}, & N > 0, \\ s_r^0\left(\dfrac{\varepsilon_y}{2\rho}\left(\dfrac{R_*}{R_0}\right)^3\right) + \dfrac{2}{3}\sigma_y\left\{\log\left(\dfrac{R_*}{R_0}\right)^3 + 1 - \left(\dfrac{R_*}{R}\right)^3\right\}, & N = 0. \end{cases} \tag{40}$$

The circumferential stress component then follows from $(27)_2$ with S_{eq} now taken as a function of R_*/R since $2\varepsilon/\varepsilon_y = (R_*/R)^3$. The formulae yield the stress components $S_{rr}, S_{\theta\theta}$ in terms of the load σ and the radius R provided they are coupled to the (39). Similarly, the radial and circumferential stress in the plastic zone of the matrix with elasto-plastic boundary at R_* follows from (27),

$$S_{rr}(R,R_*) = \begin{cases} s_r^0\left(\dfrac{\varepsilon_y}{2\rho}\left(\dfrac{R_*}{R_0}\right)^3\right) + \dfrac{2}{3}\sigma_y\dfrac{1}{N}\left[\left(\dfrac{R_*}{R_0}\right)^{3N} - \left(\dfrac{R_*}{R}\right)^{3N}\right], & N>0, \\ s_r^0\left(\dfrac{\varepsilon_y}{2\rho}\left(\dfrac{R_*}{R_0}\right)^3\right) + \dfrac{2}{3}\sigma_y\log\left(\dfrac{R}{R_0}\right)^3, & N=0. \end{cases} \tag{41}$$

Fig. 9 is a plot of the normalized circumferential stress $(S_{\theta\theta}/\sigma_y)$ at the interface versus normalized boundary traction (σ/σ_y) for different values of strain hardening coefficient N. As described above, the range of R_*/R_0 used to obtain the curves in Fig. 9 is $(1, c^{-1/3})$, i.e., initial application of the load through the point where the matrix is fully plastic. The initial portion of the curve describes elastic but non-linear response prior to yield at the interface. This is because of non-linear separation at the interface. After initial yield, the stress initially increases for all values of the hardening exponent $N \in [0,1]$. For the values of N (<1) used in the figure, $S_{\theta\theta}$ drops abruptly at bifurcation with the severity of the drop increasing with decreasing hardening coefficient. This is in contrast to elastic response, where $S_{\theta\theta}$ increases as the interface unloads.

Finally, the displacement field $u_r(R)$ in a matrix with elasto-plastic boundary at R_* may be obtained from the following:

$$u_r(R) = R\varepsilon = \varepsilon_* R\left(\frac{R_*}{R}\right)^3 = \frac{1}{2}\varepsilon_y R\left(\frac{R_*}{R}\right)^3, \tag{42}$$

which, due to the constraint of incompressibility, applies in both elastic and plastic zones. Naturally, displacement (42) must be coupled to (39) in order to obtain it as a function of load σ.

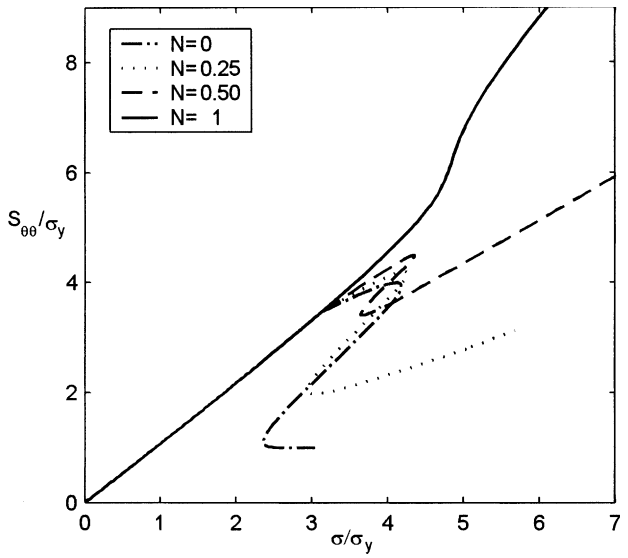

Fig. 9. Circumferential stress versus load. (Data as in Fig. 6.)

3. Non-symmetric incremental equilibrium states

3.1. The bifurcation problem

At some stage in the spherically symmetric deformation process just considered, we expect non-symmetric deformations to initiate, coincident with the rigid displacement of the inclusion within a matrix cavity. In Levy (2002), aspects of this problem were analyzed by applying the theory of incremental strain superposed on a finite deformation, to a composite sphere consisting of a hyperelastic matrix shell which separates non-linearly from a rigid inclusion. Here we apply some of the results of that work to the infinitesimal, initially strained composite sphere consisting of power law matrix material, rigid inclusion and interface characterized by a non-linear force separation relation. In the subsection that follows this one, we present an energy analysis of stability of spherically symmetric states to non-symmetrical rigid body mode perturbations. Throughout, we will maintain the assumption that the interface force law contains an additional non-dimensional length parameter of the same order of magnitude as the yield strain. Because we are dealing with a spherically symmetric initially strained state and a superposed non-symmetrical incremental state which are both infinitesimal, we normalize all strains with respect to either the yield strain or the interface force length parameter, and take the normalized initially strained state as finite and the normalized, superposed state as infinitesimal.

Without loss of generality assume that non-symmetrical configurations are characterized by fields that are independent of longitudinal angle φ. This assumption is consistent with a rigid inclusion displacement in the $\mathbf{e}_3$ direction. The superimposed infinitesimal displacement field may then be written as $\mathbf{u}_\varepsilon(\mathbf{x_0}) = u_r^\varepsilon \mathbf{e_r} + u_\theta^\varepsilon \mathbf{e_\theta}$ where the symbol ε indicates that the field is normalized with respect to yield strain ε_y. Coupled linear differential equations governing the displacement components u_r^ε, u_θ^ε and the incremental pressure $\Delta\pi$ follow from the incremental equilibrium equations (Truesdell and Noll, 1965) and the incompressibility constraint. They are given explicitly in Ogden (1984) for the case of a pressurized spherical shell, and more recently in Levy (2002) for the radially loaded composite sphere. In both of these cases, the initially strained state is finite and the matrix is hyperelastic. Now the linearity of the incremental equations indicates that the solution may be represented by an eigenfunction expansion. The radial displacement u_r^ε and incremental pressure $\Delta\pi$ are chosen to be even functions of θ while angular displacement u_θ^ε is chosen to be an odd function of θ. We can then write the solution in the form of an expansion of Legendre polynomials $P_n(\cos\theta)$,

$$\begin{aligned} u_r^\varepsilon &= U_0^\varepsilon(r) + \sum_{n=1}^{\infty} U_n^\varepsilon(r) P_n(\cos\theta), \\ u_\theta^\varepsilon &= \sum_{n=1}^{\infty} V_n^\varepsilon(r) P_n'(\cos\theta), \\ \Delta\pi &= \Pi_0(r) + \sum_{n=1}^{\infty} \Pi_n(r) P_n(\cos\theta), \end{aligned} \tag{43}$$

where $P_n'(\cos\theta) = \mathrm{d}P_n(\cos\theta)/\mathrm{d}\theta$. Ogden (1984) has shown that the expansion (43) ultimately reduces the incremental partial differential equations to a single fourth order equation for $U_n^\varepsilon(r)$ and two other equations giving $V_n^\varepsilon(r), \Pi_n(r)$ in terms of it. For the $n = 0, 1$ modes he has integrated the fourth order equation exactly. Because we have considered the spherically symmetric $n = 0$ mode in the previous section here we focus on the first non-symmetric $n = 1$ mode. Thus,

$$r\ddot{U}_1^\varepsilon + (\lambda^3 + 3)\dot{U}_1^\varepsilon = \frac{C_1 r}{\lambda \varepsilon_y \beta}, \quad r^4 \dot{U}_1^\varepsilon = 2C_1 \lambda \int^r t^4 \frac{\lambda^3 - \lambda^{-3}}{\mathrm{D}\hat{w}(\lambda)}\,\mathrm{d}t + \lambda C_2, \tag{44}$$

where a dot indicates derivative with respect to coordinate r and β is defined by

$$\beta = \frac{\lambda}{2(\lambda^6 - 1)} \mathrm{D}\hat{w}(\lambda),$$

which we take to be positive by virtue of the Baker–Ericksen inequalities. The quantity $V_1^\varepsilon(r)$ is determined from

$$V_1^\varepsilon = \frac{1}{2}(r\dot{U}_1^\varepsilon + 2U_1^\varepsilon). \tag{45}$$

Result (44) presumes that the initially strained state is finite. In our case the initially strained spherically symmetric state is infinitesimal but the normalized state, characterized by $\varepsilon/\varepsilon_y$ $(= (\lambda - 1)/\varepsilon_y)$, is finite. Therefore, we can write (44) in the form

$$r\ddot{U}_1^\varepsilon + 4\dot{U}_1^\varepsilon = 12C_1 r \frac{\varepsilon/\varepsilon_y}{\mathrm{D}\hat{w}(\varepsilon/\varepsilon_y)}, \quad r^4\dot{U}_1^\varepsilon = 12C_1 \int^r t^4 \frac{\varepsilon/\varepsilon_y}{\mathrm{D}\hat{w}(\varepsilon/\varepsilon_y)}\,\mathrm{d}t + C_2, \tag{46}$$

which, by (21)–(23), can be integrated directly.

In the finite initially strained problem the boundary conditions consist of a spherically symmetric dead load traction applied to the outer surface of the composite sphere and a configuration dependent interface traction, $\mathbf{s_I}(-\mathbf{e_r}) = -s_r\mathbf{e_r} - s_\theta\mathbf{e_\theta}$, applied to the inner boundary of the composite spherical shell. The arguments of s_r, s_θ are the ratios of the normalized (with respect to inclusion radius) interface displacement jump components $\tilde{u}, \tilde{v}$ to force length parameter ρ. (Note that $s_r(\varepsilon_0/\rho, 0) = s_r^0(\varepsilon_0/\rho)$ introduced previously.) As shown in Levy (2002) the boundary conditions can be expressed in terms of the mode multipliers which, for the $n = 1$ mode, are

$$\begin{aligned}
&\varepsilon_y\beta(\lambda_1)r_1\ddot{U}_1^\varepsilon(r_1) + [2\beta(\lambda_1) + \lambda_1^{-2}\sigma]\varepsilon_y\dot{U}_1^\varepsilon(r_1) = 0,\\
&\varepsilon_y\beta(\lambda_0)r_0\ddot{U}_1^\varepsilon(r_0) + 2\varepsilon_y\beta(\lambda_0)\dot{U}_1^\varepsilon(r_0) = \frac{3}{2}\int_0^\pi s_r P_1(\cos\theta)\sin\theta\,\mathrm{d}\theta.
\end{aligned} \tag{47}$$

For infinitesimal initially strained states, but finite normalized states, (47) assumes the form

$$\begin{aligned}
&r_1\ddot{U}_1^\varepsilon(r_1) + 2\dot{U}_1^\varepsilon(r_1) = 0,\\
&\hat{\beta}(\varepsilon_0/\varepsilon_y)r_0\ddot{U}_1^\varepsilon(r_0) + 2\hat{\beta}(\varepsilon_0/\varepsilon_y)\dot{U}_1^\varepsilon(r_0) = \mathrm{D}_{\tilde{u}/\rho}s_r(\varepsilon_0/\rho, 0)\frac{\varepsilon_y}{\rho}\frac{U_1^\varepsilon(r_0) - w^\varepsilon}{r_0},
\end{aligned} \tag{48}$$

where $\hat{\beta} = \mathrm{D}\hat{w}(\varepsilon/\varepsilon_y)/(12\varepsilon/\varepsilon_y)$ and we note that the ratio of yield strain to force length parameter is finite since it is assumed that they are of the same order of magnitude. The quantity w^ε is the magnitude of a rigid body displacement in the $\mathbf{e}_3$ direction and it appears in (48) because the interface force s_r depends on the difference between the inner matrix boundary displacement and the rigid body displacement of the (rigid) inclusion (for a more detailed description of the kinematics see Levy (2002)). (Note that we are assuming that the inclusion does not rotate in the superimposed deformation.)

An additional constraint on the rigid body displacement arises from overall rigid body equilibrium of the inclusion. It can be shown (Levy, 2002) that the single non-trivial equilibrium equation is of the form

$$\int_0^\pi [s_r P_1(\cos\theta) + s_\theta P_1'(\cos\theta)]\sin\theta\,\mathrm{d}\theta = 0, \tag{49}$$

which is valid for finite initially strained states. For infinitesimal initially strained states (49) may be written as

$$\mathrm{D}_{\tilde{u}/\rho}s_r(\varepsilon_0/\rho, 0)\frac{U_1^\varepsilon(r_0) - w^\varepsilon}{r_0} + 2\mathrm{D}_{\tilde{v}/\rho}s_\theta(\varepsilon_0/\rho, 0)\frac{V_1^\varepsilon(r_0) - w^\varepsilon}{r_0} = 0, \tag{50}$$

where we have used the fact that the ratio of the normalized (with respect to inclusion radius) interface displacement jump components to force length parameter are

$$\begin{aligned}\frac{\tilde{u}(r_0,\theta)}{\rho} &= \frac{\varepsilon_0}{\rho}+\frac{\varepsilon_y}{\rho}\frac{U_0^{\varepsilon}(r_0)}{r_0}+\frac{\varepsilon_y}{\rho}\frac{U_1^{\varepsilon}(r_0)-w^{\varepsilon}}{r_0}P_1(\cos\theta)+\cdots,\\ \frac{\tilde{v}(r_0,\theta)}{\rho} &= \frac{\varepsilon_y}{\rho}\frac{V_1^{\varepsilon}(r_0)-w^{\varepsilon}}{r_0}P_1'(\cos\theta)+\cdots\end{aligned} \tag{51}$$

Note that (51) follows from the fact that the normalized displacement jump components $\tilde{u},\tilde{v}$ from the undeformed state to the current configuration arise from the superposition of the deformation ε_0 of the spherically symmetric initially strained state, plus the superposed non-symmetrical deformation $u_r/R_0, u_\theta/R_0$ minus the rigid body displacement of the inclusion w_0/R_0. In obtaining (51), we have employed (43) and additionally, we have assumed that initially strained equilibrium states are infinitesimal. Boundary conditions (48), rigid body equilibrium constraint (50) and general solution (46) may be used to predict aspects of the $n=1$ bifurcation mode and the critical load at which it occurs. In what follows, we consider two cases, the composite sphere with a smooth interface, and an unbounded matrix allowing for interfacial shear.

The smooth interface. When the interface is smooth it cannot support shear traction and $s_\theta = 0$ and s_r is independent of $\tilde{v}$ (in which case we write $s_r(\tilde{u}/\rho)$). In this case (50) becomes $\mathrm{D}_{\tilde{u}/\rho}s_r(\varepsilon_0/\rho)\times[(U_1^{\varepsilon}(r_0)-w^{\varepsilon})/r_0]=0$ and boundary conditions (48) become homogeneous,

$$\begin{aligned} &r_1\ddot{U}_1^{\varepsilon}(r_1)+2\dot{U}_1^{\varepsilon}(r_1)=0,\\ &r_0\ddot{U}_1^{\varepsilon}(r_0)+2\dot{U}_1^{\varepsilon}(r_0)=0.\end{aligned} \tag{52}$$

The solution $(46)_2$ together with boundary conditions (52) imply that C_2 is linearly related to C_1 and

$$\left[\int_{c\Gamma_0}^{\Gamma_0}\frac{\Gamma^{-2/3}\mathrm{D}^2\hat{w}(\Gamma)}{[\mathrm{D}\hat{w}(\Gamma)]^2}\,\mathrm{d}\Gamma\right]C_1=0, \tag{53}$$

where an integration by parts has been carried out and we recall that $\Gamma_0=\varepsilon_0/\varepsilon_y$. It is not hard to show that for $\hat{w}$ defined by (20) the integral in (53) is generally non-zero and of one sign. The exception is in the limit of the non-hardening matrix ($N\downarrow 0$), as the matrix shell becomes fully plastic. This is readily apparent from the expansion of the integral for the case of a partially plastic power law matrix shell with $\Gamma_0\geqslant 1/2$ and $c\Gamma_0\leqslant 1/2$,

$$\int_{c\Gamma_0}^{\Gamma_0}\frac{\Gamma^{-2/3}\mathrm{D}^2\hat{w}(\Gamma)}{[\mathrm{D}\hat{w}(\Gamma)]^2}\,\mathrm{d}\Gamma=\frac{3}{20\sigma_y}\left[(c\Gamma_0)^{-5/3}-\left(\frac{1}{2}\right)^{-5/3}\right]+\frac{3\cdot 2^{-(N+1)}N}{(2+3N)\sigma_y}\left[\left(\frac{1}{2}\right)^{-2/3-N}-(\Gamma_0)^{-2/3-N}\right].$$

Excluding this exceptional case we have that (53) implies that C_1, and therefore C_2, is zero. Then by $(46)_2$ U_1^{ε}, and therefore V_1^{ε} $(=U_1^{\varepsilon})$, is a constant to be absorbed into the unknown rigid body displacement w^{ε}. The rigid body constraint (50) then becomes

$$\mathrm{D}_{\tilde{u}/\rho}s_r(\varepsilon_0/\rho)\frac{w^{\varepsilon}}{r_0}=0. \tag{54}$$

Mode $n=1$ bifurcation phenomena characterizing the first non-symmetric mode is therefore governed by (54). The spherically symmetric bifurcation mode $n=0$, which has been analyzed in detail in the first part of the paper, is governed by

$$\mathrm{D}_{\varepsilon_0}F(\varepsilon_0,\sigma)\frac{U_0^{\varepsilon}}{r_0}=\Delta\sigma, \tag{55}$$

where U_0^{ε} is the incremental spherically symmetric mode multiplier, $\Delta\sigma$ is the incremental loading and $\mathrm{D}_{\varepsilon_0}F(\varepsilon_0,\sigma)$ is given by (30) or (31). Non-symmetrical solutions $w^{\varepsilon}\neq 0$ associated with (54) and (55) exist provided,

$$\mathrm{D}_{\vec{u}/\rho}s_r(\varepsilon_0/\rho)=0, \tag{56}$$

that is, when the interface force obtains its maximum value. (Note that the eigenmode is the non-symmetric rigid body displacement $w^{\varepsilon}(\cos\theta\mathbf{e}_r-\sin\theta\mathbf{e}_\theta)$, which is orthogonal to the incremental load as required.) For an interface force law with $s_r=s_r^0$ and s_r^0 given by (33) the maximum occurs when $\varepsilon_0=\rho$ so that $s_r(1)=\sigma_{\max}$. Recall that we have shown previously that when the matrix is composed of hardening material or, when it is non-hardening and not fully plastic, spherically symmetric bifurcation occurs when $\mathrm{D}_{\vec{u}/\rho}s_r(\varepsilon_0/\rho)<0$. Thus, (56) implies that non-symmetric bifurcation always precedes spherically symmetric bifurcation unless the material is non-hardening and fully plastic in which case they coincide. Furthermore, unlike spherically symmetric bifurcation, there is no threshold value of N so that non-symmetric bifurcation will always occur. Now recall (25) for the power law matrix. The critical load at bifurcation is

$$\sigma=\begin{cases}\sigma_{\max}+\dfrac{4}{3}(1-c)\sigma_y\dfrac{\rho}{\varepsilon_y}, & \dfrac{2\rho}{\varepsilon_y}\leqslant 1,\\[2ex] \sigma_{\max}+\dfrac{2}{3}\sigma_y\left\{\dfrac{1}{N}\left[\left(\dfrac{2\rho}{\varepsilon_y}\right)^N-1\right]+1-c\dfrac{2\rho}{\varepsilon_y}\right\}, & \dfrac{2c\rho}{\varepsilon_y}\leqslant 1\leqslant\dfrac{2\rho}{\varepsilon_y},\\[2ex] \sigma_{\max}+\dfrac{2}{3}\dfrac{\sigma_y}{N}(1-c^N\left(\dfrac{2\rho}{\varepsilon_y}\right)^N, & 1\leqslant\dfrac{2c\rho}{\varepsilon_y}\leqslant\dfrac{2\rho}{\varepsilon_y}.\end{cases} \tag{57}$$

For the non-hardening matrix the result is

$$\sigma=\begin{cases}\sigma_{\max}+\dfrac{4}{3}(1-c)\sigma_y\dfrac{\rho}{\varepsilon_y}, & \dfrac{2\rho}{\varepsilon_y}\leqslant 1,\\[2ex] \sigma_{\max}+\dfrac{2}{3}\sigma_y\left[\log\left(\dfrac{2\rho}{\varepsilon_y}\right)+1-c\dfrac{2\rho}{\varepsilon_y}\right], & \dfrac{2c\rho}{\varepsilon_y}\leqslant 1\leqslant\dfrac{2\rho}{\varepsilon_y},\\[2ex] \sigma_{\max}+\dfrac{2}{3}\sigma_y\log c^{-1}, & 1\leqslant\dfrac{2c\rho}{\varepsilon_y}\leqslant\dfrac{2\rho}{\varepsilon_y}.\end{cases} \tag{58}$$

Because the terms on the right-hand side (57) and (58) are positive we have the fact that non-symmetric bifurcation always occurs at a value of applied load which is greater than the interface strength. Fig. 10 is a plot of normalized bifurcation load (σ/σ_y) versus normalized force length parameter (ρ/ε_y) for different values of strain hardening coefficient N. The data used in the figure coincides with that used in previous figures, i.e., $\sigma_{\max}=3\sigma_y$, $c=0.0104$. The behavior is bounded by the elastic case $(N=1)$ and the non-hardening case $(N=0)$. As expected increasing the force length parameter increases the bifurcation load. Increasing the strain hardening coefficient has the effect of elevating the bifurcation load as well. As is apparent from (57) and (58) increasing the interface strength also increases the bifurcation load.

The unbounded matrix; interfacial shear. The unbounded matrix is characterized by a vanishing concentration c. The boundary conditions (48) and the rigid body equilibrium condition (50) remain valid for this case provided we apply $(48)_1$ remotely, i.e., as $r_1\uparrow\infty$. If we assume that $\dot{U}_1^{\varepsilon}$ remains bounded as $r_1\uparrow\infty$ then $(48)_1$ and $(46)_1$ imply that $C_1=0$. It follows from $(46)_2$ that

$$\ddot{U}_1^{\varepsilon}=-4C_2r^{-5},\quad \dot{U}_1^{\varepsilon}=C_2r^{-4},\quad U_1^{\varepsilon}=-\frac{1}{3}C_2r^{-3}+C_3. \tag{59}$$

The interface boundary condition $(48)_2$ determines C_2, which in turn fixes $U_1^{\varepsilon}, V_1^{\varepsilon}$ in terms of C_3 and w_0^{ε}. The bifurcation condition is then determined by substituting these values of $U_1^{\varepsilon}, V_1^{\varepsilon}$ into (50). The result is

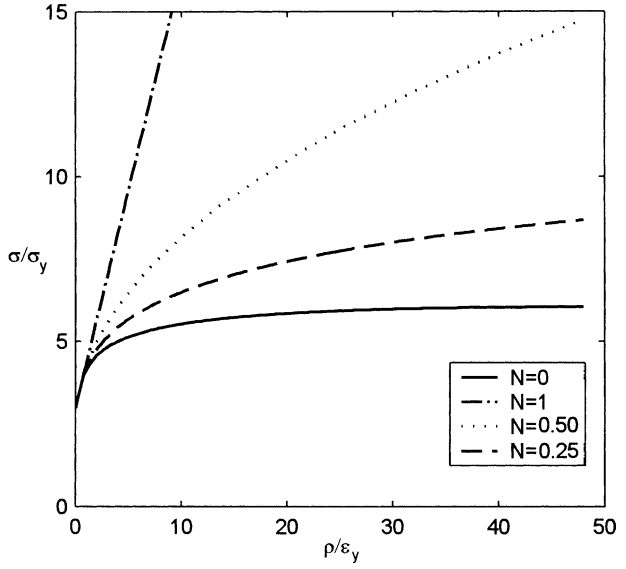

Fig. 10. Critical load versus force length parameter. Smooth interface. $\sigma_{\max} = 3\sigma_y$, $c = 0.0104$.

$$\frac{C_3 - w_0^{\varepsilon}}{r_0}[(1+\alpha)\mathrm{D}_{\tilde{u}/\rho}s_r(\varepsilon_0/\rho,0) + 2(1-\alpha/2)\mathrm{D}_{\tilde{v}/\rho}s_\theta(\varepsilon_0/\rho,0)] = 0, \tag{60}$$

where α is given by

$$\alpha = \frac{(\varepsilon_y/\rho)\mathrm{D}_{\tilde{u}/\rho}s_r(\varepsilon_0/\rho,0)/4\hat{\beta}}{1-(\varepsilon_y/\rho)\mathrm{D}_{\tilde{u}/\rho}s_r(\varepsilon_0/\rho,0)/4\hat{\beta}}. \tag{61}$$

In this paper, we will assume that at bifurcation the quantity α is so small that it can be neglected in comparison to unity (so that $U_1^{\varepsilon} = V_1^{\varepsilon} = \text{constant}$). In order to see the consequence of this assumption recall that when there is no interfacial shear the interface force law is such that $s_r(\varepsilon_0/\rho)$ is a maximum when $\varepsilon_0/\rho = 1$ which is the bifurcation condition for the smooth interface. Now assume that with interfacial shear present, bifurcation occurs when $\varepsilon_0/\rho = 1+\delta$ where δ is a small parameter. Then $\mathrm{D}_{\tilde{u}/\rho}s_r(1+\delta,0) = \mathrm{O}(\delta)$, $\alpha = \mathrm{O}(\delta)$ and $\mathrm{D}_{\tilde{v}/\rho}s_\theta(1+\delta,0) = \mathrm{O}(\delta)$. (Note that we are assuming that $\mathrm{D}_{\tilde{u}/\rho}s_r(\varepsilon_0/\rho,0) = \mathrm{D}_{\tilde{u}/\rho}s_r(\varepsilon_0/\rho)$, i.e., that the slope of the force law for spherically symmetric states is equal to the slope of the force law for the smooth interface.) By neglecting α we are neglecting terms of order $\mathrm{O}(\delta^2)$ compared to terms of order $\mathrm{O}(\delta)$ in (60). This is consistent with an interfacial shear stiffness of order $\mathrm{O}(\delta)$ (see (64)). The rigid body constraint condition then simplifies to

$$[\mathrm{D}_{\tilde{u}/\rho}s_r(\varepsilon_0/\rho,0) + 2\mathrm{D}_{\tilde{v}/\rho}s_\theta(\varepsilon_0/\rho,0)]\frac{w^{\varepsilon}}{r_0} = 0, \tag{62}$$

where C_3 has been absorbed into w_0^{ε}. Mode $n = 1$ bifurcation phenomena characterizing the first non-symmetric mode is therefore governed by (62) which is a generalization of (54). Non-symmetric solutions $w^{\varepsilon} \neq 0$ associated with (55) and (62) exist provided

$$\mathrm{D}_{\tilde{u}/\rho}s_r(\varepsilon_0/\rho,0) + 2\mathrm{D}_{\tilde{v}/\rho}s_\theta(\varepsilon_0/\rho,0) = 0 \tag{63}$$

with rigid body eigenmode $w^{\varepsilon}(\cos\theta\mathbf{e}_r - \sin\theta\mathbf{e}_\theta)$.

To obtain explicit results consider a modification of the normal exponential force-separation law (33) to account for interfacial shear (Needleman, 1992),

$$\begin{aligned} s_r(\tilde{u}/\rho, \tilde{v}/\rho) &= e\sigma_{\max}\left\{\frac{\tilde{u}}{\rho} - \frac{1}{2}\eta\left(\frac{\tilde{v}}{\rho}\right)^2\right\}\mathrm{e}^{-\tilde{u}/\rho}, \\ s_\theta(\tilde{u}/\rho, \tilde{v}/\rho) &= e\sigma_{\max}\left\{\eta\frac{\tilde{v}}{\rho}\right\}\mathrm{e}^{-\tilde{u}/\rho}, \end{aligned} \tag{64}$$

where interfacial shear parameter η ($\geqslant 0$) is a measure of both the shear stiffness of the interface as well as the strength of the coupling between the normal and tangential separation modes. The parameters $\sigma_{\max}$ and ρ retain the same meaning as defined previously. This simple model characterizes non-linear normal separation and linear shear slip appropriate for incipient non-symmetrical branching from the principal path of spherically symmetric equilibrium states.

For the force law (64), bifurcation condition (63) becomes

$$\frac{\varepsilon_0^*}{\rho} = 1 + 2\eta. \tag{65}$$

Critical loads for non-symmetric bifurcation are obtained by substituting (65) into (25), for the power law matrix, and (26) for the non-hardening matrix. For the power law matrix the result is

$$\sigma = \begin{cases} \sigma_{\max}(1+2\eta)\mathrm{e}^{-2\eta} + \dfrac{4}{3}E\rho(1+2\eta), & \dfrac{2\rho(1+2\eta)}{\varepsilon_y} \leqslant 1, \\ \sigma_{\max}(1+2\eta)\mathrm{e}^{-2\eta} + \dfrac{2}{3}\sigma_y\left\{\dfrac{1}{N}\left[\left(\dfrac{2\rho(1+2\eta)}{\varepsilon_y}\right)^N - 1\right] + 1\right\}, & 1 \leqslant \dfrac{2\rho(1+2\eta)}{\varepsilon_y}, \end{cases} \tag{66}$$

while for the non-hardening matrix

$$\sigma = \begin{cases} \sigma_{\max}(1+2\eta)\mathrm{e}^{-2\eta} + \dfrac{4}{3}E\rho(1+2\eta), & \dfrac{2\rho(1+2\eta)}{\varepsilon_y} \leqslant 1, \\ \sigma_{\max}(1+2\eta)\mathrm{e}^{-2\eta} + \dfrac{2}{3}\sigma_y\left[\log\left(\dfrac{2\rho(1+2\eta)}{\varepsilon_y}\right) + 1\right], & 1 \leqslant \dfrac{2\rho(1+2\eta)}{\varepsilon_y}. \end{cases} \tag{67}$$

Eqs. (66) and (67) extend the smooth interface results (57) and (58) (with $c = 0$) to account for interfacial shear. Note that non-symmetric bifurcation always occurs at a critical load that exceeds the interface force $s_r(\varepsilon_0^*/\rho, 0) = \sigma_{\max}(1+2\eta)\mathrm{e}^{-2\eta}$.

Fig. 11 is a plot of normalized bifurcation stress (σ/σ_y) versus normalized force length parameter (ρ/ε_y) for different values of interfacial shear parameter (η). The data used in the figure is $\sigma_{\max} = 3\sigma_y$, $N = 0.1$ which coincides with that used in previous figures. As expected, the critical load increases with force length parameter. The effect of interfacial shear parameter on behavior is not as obvious. For the range of ρ/ε_y values depicted in the figure no discernable trend is observed. If this range is substantially increased then the $\eta = 1$ curve will cross the $\eta = 0, 0.1$ curves and we will have the result that ultimately, increasing the interfacial shear parameter raises the bifurcation stress. For small values of ρ/ε_y (not indicated in the figure) the opposite trend is observed, i.e., increasing η decreases the bifurcation load. This unphysical result has been described in Levy (2001, 2002) and is a consequence of the global structure of branches of equilibria emanating from the principal spherically symmetric one. Essentially those bifurcation points, for which increasing η decreases the critical load, lie on unstable branches which are unreachable by a continuous increase in load from the undeformed state. The numerical determination of the non-symmetrical branches of equilibrium states is beyond the scope of this paper. This kind of calculation however has been carried out in Levy (1998) for the case where the matrix and the inclusion are linear elastic.

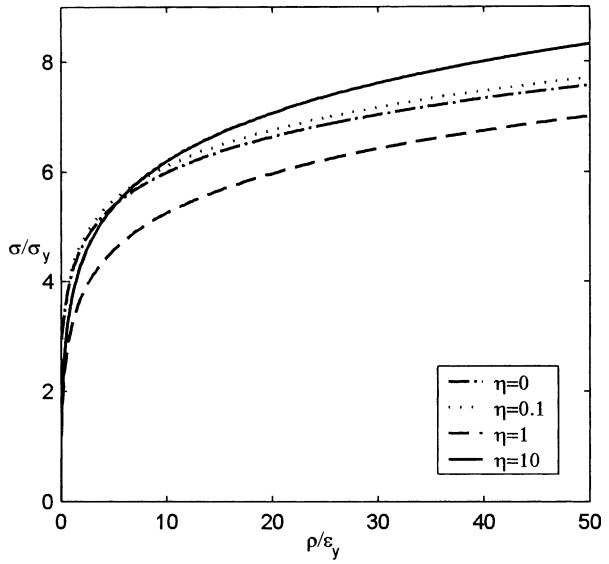

Fig. 11. Critical load versus force length parameter. Unbounded matrix. $\sigma_{\max} = 3\sigma_y$, $N = 0.1$.

3.2. The stability problem

Here we focus on the composite sphere with a smooth interface and the unbounded matrix with interfacial shear (subject to the restriction that α is small). Recall that for these two cases, the $n = 1$ mode $U_1^{\varepsilon}P_1(\cos\theta), V_1^{\varepsilon}P_1'(\cos\theta)$ vanishes so that the strain energy of the matrix will be independent of this mode. We begin by constructing the potential energy associated with a deformed state of the sphere obtained by subjecting the finite spherically symmetric state to superimposed, infinitesimal spherically symmetric and non-symmetric rigid body perturbations. The potential energy for the infinitesimally strained power law matrix will then be obtained by a formal limit process. Now the potential energy Φ consists of the strain energy of the matrix, the interface energy associated with normal separation mode and shear slip mode, and the potential energy of the loading. The first and third terms on the right-hand side of (14) representing the strain energy of the matrix and the potential energy of the loading are essentially unchanged provided we substitute for f the deformation $\tilde{f} = f + U_0$ where U_0 represents the infinitesimal spherically symmetric perturbation. The interface energy is given by

$$\int_{t_0}^{t_1} \left\{ \int_{\partial \mathbf{f}(\Omega)} \mathbf{s_I}(-\mathbf{e_r}) \cdot [\mathbf{v}] \, \mathrm{d}A \right\} \mathrm{d}t,$$

where $[\mathbf{v}]$ is the velocity of points on the inner matrix boundary relative to the inclusion $[\mathbf{v}] = \dot{\tilde{f}}\mathbf{e}_r - \dot{w}_0(\cos\theta\mathbf{e}_r - \sin\theta\mathbf{e}_\theta)$, i.e., the velocity jump at the interface neglecting all modes higher than $n = 1$. Note that here a superposed dot indicates time derivative. The potential energy can be written in the final form

$$\begin{aligned}\widehat{\Phi}(u_0,\omega_0) = {} & 3c[(\lambda_0+u_0)^3 - 1] \int_{[1+c((\lambda_0+u_0)^3-1)]^{1/3}}^{\lambda_0+u_0} \frac{\hat{\sigma}(\lambda^{-2},\lambda,\lambda)\lambda^2}{(\lambda^3-1)^2}\,\mathrm{d}\lambda - 3\sigma\{[1+c((\lambda_0+u_0)^3-1)]^{1/3} - 1\} \\ & + 3c\int^{\lambda_0+u_0} \hat{s}_r^0(z) z^2\,\mathrm{d}z + \frac{c}{\rho}\left[\mathrm{D}_{\dot{u}/\rho} s_r\left(\frac{\lambda_0-1}{\rho},0\right) + 2\mathrm{D}_{\dot{v}/\rho} s_\theta\left(\frac{\lambda_0-1}{\rho},0\right)\right](\lambda_0+u_0)^2 \int^{\omega_0} z\,\mathrm{d}z,\end{aligned} \tag{68}$$

where $u_0 = U_0(R_0)/R_0$ is now the normalized spherically symmetric perturbation, $\omega_0 = w_0/R_0$ is the normalized non-symmetrical rigid body perturbation and $\widehat{\boldsymbol{\Phi}}$ has been normalized with respect to the sphere volume $\frac{4}{3}\pi R_1^3$. [2] (Recall that $\hat{s}_r^0(\lambda_0) = s_r^0((\lambda_0 - 1)/\rho)$ is the normal component of interface force for spherically symmetric states.)

It is a straightforward matter to show that values of u_0, which render $\widehat{\boldsymbol{\Phi}}$ stationary for vanishing ω_0, are solutions to the equation governing continuing spherically symmetric equilibrium

$$\begin{aligned} 0 &= \mathrm{D}_{u_0}\widehat{\boldsymbol{\Phi}}(u_0, 0) \\ &= 3c\lambda_0^2\lambda_1^{-2}\left\{ -\Delta\sigma + \left[\frac{-\lambda_0^3 \mathrm{D}_\lambda \hat{w}(\lambda_1)}{(\lambda_0^3 - 1)} + \frac{\lambda_0\lambda_1^2 \mathrm{D}_\lambda \hat{w}(\lambda_0)}{(\lambda_0^3 - 1)} + 2c\sigma\lambda_0^3\lambda_1^{-3} + \lambda_0\lambda_1^2\rho^{-1}\mathrm{D}_{\tilde{u}/\rho}s_r\left(\frac{\lambda_0 - 1}{\rho}, 0\right)\right]\frac{U_0(r_0)}{r_0}\right\}, \end{aligned} \tag{69}$$

where terms of order $\mathrm{O}(u_0^2)$ have been neglected and use has been made of (10) and (3). This equation has been obtained by Levy (2002) by expanding (10) in a series of small perturbations about λ_0. Consider now the derivative $\mathrm{D}_{\omega_0}\widehat{\boldsymbol{\Phi}}(u_0, \omega_0)$. By neglecting terms of second order in u_0, ω_0 we have

$$\mathrm{D}_{\omega_0}\widehat{\boldsymbol{\Phi}}(0, \omega_0) = \frac{c}{\rho}\lambda_0^2\left[\mathrm{D}_{\tilde{u}/\rho}s_r\left(\frac{\lambda_0 - 1}{\rho}, 0\right) + 2\mathrm{D}_{\tilde{v}/\rho}s_\theta\left(\frac{\lambda_0 - 1}{\rho}, 0\right)\right]\omega_0, \tag{70}$$

so that $\widehat{\boldsymbol{\Phi}}$ is stationary for all values of ω_0 provided the bracketed quantity in (70) vanishes. This is identical to the equation governing the rigid body bifurcation mode ω_0 (Levy, 2002).

The second derivatives of $\widehat{\boldsymbol{\Phi}}$ are required to assess the stability of spherically symmetric equilibrium states to both spherically symmetric and non-symmetric rigid body perturbations. They are given by

$$\begin{aligned} &\mathrm{D}_{u_0}^2\widehat{\boldsymbol{\Phi}}(0,0) = 3c\lambda_0\lambda_1^{-5}\left[2c\sigma\lambda_0^3 + \lambda_0\lambda_1^5\rho^{-1}\mathrm{D}_{\tilde{u}/\rho}s_r\left(\frac{\lambda_0 - 1}{\rho}, 0\right) - \frac{\lambda_0^3\lambda_1^3\mathrm{D}_\lambda\hat{w}(\lambda_1)}{(\lambda_0^3 - 1)} + \frac{\lambda_0\lambda_1^5\mathrm{D}_\lambda\hat{w}(\lambda_0)}{(\lambda_0^3 - 1)}\right], \\ &\mathrm{D}_{u_0,\omega_0}\widehat{\boldsymbol{\Phi}}(0,0) = 0, \\ &\mathrm{D}_{\omega_0}^2\widehat{\boldsymbol{\Phi}}(0,0) = \frac{c}{\rho}\lambda_0^2\left[\mathrm{D}_{\tilde{u}/\rho}s_r\left(\frac{\lambda_0 - 1}{\rho}, 0\right) + 2\mathrm{D}_{\tilde{v}/\rho}s_\theta\left(\frac{\lambda_0 - 1}{\rho}, 0\right)\right]. \end{aligned} \tag{71}$$

Thus, the spherically symmetric equilibrium state characterized by λ_0 is locally stable if the (non-vanishing) second derivatives in (71) are positive for all infinitesimal perturbations u_0, ω_0. Note that $\mathrm{D}_{u_0}^2\widehat{\boldsymbol{\Phi}}(0,0)$ given by $(71)_1$ is identical to (16) so that $\mathrm{D}_{u_0}^2\widehat{\boldsymbol{\Phi}}(0,0) > 0$ is sufficient to insure local stability to spherically symmetric perturbations. (This result follows by specializing (5) to be $\lambda_1^3 - 1 = c(\lambda_0^3 - 1)$.) The condition $\mathrm{D}_{\omega_0}^2\widehat{\boldsymbol{\Phi}}(0,0) > 0$ therefore guarantees local stability to non-symmetric rigid body perturbations.

Consider first the smooth interface, $s_\theta(\tilde{u}/\rho, \tilde{v}/\rho) = 0$, s_r independent of $\tilde{v}$. Then stability to non-symmetric perturbations requires that

$$\mathrm{D}_{\omega_0}^2\widehat{\boldsymbol{\Phi}}(0,0) = c\rho^{-1}\lambda_0^2\mathrm{D}_{\tilde{u}/\rho}s_r\left(\frac{\lambda_0 - 1}{\rho}\right) > 0,$$

i.e., the slope of the interface force-separation curve must be positive. Thus, whereas the existence of unstable spherically symmetric equilibrium states to spherically symmetric perturbations (discussed in the first part of the paper) depends on the interface force law as well as the strain energy of the matrix, the instability to non-symmetric rigid body perturbations only requires that equilibria reside on the descending branch of the force-separation law.

[2] For the unbounded matrix multiply through by R_1^3 to avoid the difficulties arising from $R_1 \uparrow \infty$.

For the unbounded matrix, we multiply the second derivatives in (71) through by R_1^3 (recall footnote 2) and let $c = 0$, $\lambda_1 = 1$, $\mathrm{D}\hat{w}(1) = 0$ (no residual stress). In particular, stability to non-symmetric perturbations requires that

$$\lambda_0^2\left[\mathrm{D}_{\tilde{u}/\rho}s_r\left(\frac{\lambda_0-1}{\rho},0\right)+2\mathrm{D}_{\tilde{v}/\rho}s_\theta\left(\frac{\lambda_0-1}{\rho},0\right)\right]>0.$$

For the interface force law given by (64), this amounts to requiring that $\lambda_0 < 1+\rho(1+2\eta)$. Thus, the appearance of unstable, spherically symmetric equilibrium states to non-symmetric perturbations can be delayed by increasing interfacial shear stiffness (η) but not eliminated.

Results for the infinitesimally deformed power law matrix composite sphere directly parallel those for the finitely deformed hyperelastic matrix composite sphere. The potential energy for the infinitesimally deformed composite sphere may be obtained by substituting the variable $\Gamma = (\lambda-1)/\varepsilon_y = \varepsilon/\varepsilon_y$ in (68) and expanding in a series in ε_y retaining only terms linear in ε_y. As was done previously, we assume the quantities Γ and ε_y/ρ are finite for infinitesimal ε_y. The result, which may be compared with (36) the potential energy for spherically symmetric deformations, is given by

$$\begin{aligned}\widehat{\Phi}(u_\varepsilon,\omega_\varepsilon) &= c(\Gamma_0+u_\varepsilon)\int_{c(\Gamma_0+u_\varepsilon)}^{\Gamma_0+u_\varepsilon}\frac{\hat{w}(\Gamma)}{\Gamma^2}\,\mathrm{d}\Gamma+3c\varepsilon_y\int^{\Gamma_0+u_\varepsilon}s_r^0\left(\Gamma\frac{\varepsilon_y}{\rho}\right)\mathrm{d}\Gamma-3\sigma c\varepsilon_y(\Gamma_0+u_\varepsilon)\\&\quad+\frac{1}{2}c\rho^{-1}\varepsilon_y\left[\mathrm{D}_{\tilde{u}/\rho}s_r\left(\Gamma_0\frac{\varepsilon_y}{\rho},0\right)+2\mathrm{D}_{\tilde{v}/\rho}s_\theta\left(\Gamma_0\frac{\varepsilon_y}{\rho},0\right)\right]\omega_\varepsilon^2,\end{aligned}\tag{72}$$

where $u_\varepsilon, \omega_\varepsilon$ are perturbations normalized with respect to ε_y and strain energy $\hat{w}$ is given by (20). It is not difficult to show that the vanishing of the derivatives $\mathrm{D}_{u_\varepsilon}\widehat{\Phi}(u_\varepsilon,0), \mathrm{D}_{\omega_\varepsilon}\widehat{\Phi}(0,\omega_\varepsilon)$ are equivalent to the equation for continuing spherically symmetric equilibrium, and the equation governing the rigid body mode, respectively. The second derivative of (72) $\mathrm{D}^2_{u_\varepsilon}\widehat{\Phi}(0,0)$ is given by $(37)_2$, (30) and (31). The derivative $\mathrm{D}^2_{\omega_\varepsilon}\widehat{\Phi}(0,0)$ leads to the local stability condition

$$\mathrm{D}_{\tilde{u}/\rho}s_r(\varepsilon_0/\rho,0)+2\mathrm{D}_{\tilde{v}/\rho}s_\theta(\varepsilon_0/\rho,0)>0,\tag{73}$$

which, for the interface force law (64), is satisfied when $\varepsilon_0/\rho < 1+2\eta$.

4. Conclusions

In this paper, we have focused on spherically symmetric and non-symmetric bifurcation and stability phenomena associated with cavity nucleation by interfacial separation in a power law matrix composite sphere deforming at infinitesimal strain. The results obtained are applicable for the metallic material matrix provided a continuum description of the plastically deforming matrix remains valid for the composite sphere and, if we utilize the results up to initial bifurcation only. Owing to the assumed hyperelastic constitutive relation, predictions based on this model beyond critical loads are invalid due to the absence of a linear elastic unloading regime. Treatment of the non-symmetric problem beyond initial bifurcation would cause additional difficulties, other than the ones already described, owing for the need to employ an incremental flow theory for non-proportional loading in the post bifurcation regime.

Simple formulae for the critical loads required to initiate spherically symmetric and non-symmetric bifurcation have been obtained. It is physically reasonable to associate the critical load for non-symmetric bifurcation with the nucleation load. This is because non-symmetric bifurcation exists for all parameter values and its attainment signals the onset of unstable spherically symmetric equilibrium states. The linearized bifurcation analysis carried out in the second part of the paper suggests that the non-symmetric bifurcation point is a pitchfork. A number of global portraits consistent with this are then possible

including ductile decohesion accompanied by a gradual rigid body displacement of the inclusion and brittle decohesion accompanied by an abrupt displacement of the inclusion within a larger cavity. Either of these scenarios, as well as other possibilities, may reasonably be associated with the nucleation event. Furthermore, the critical load $(66)_2$, for non-symmetric bifurcation, has many of the properties we normally associate with nucleation. Namely, a critical load that (i) increases with increasing force length parameter ρ and decreasing yield strain ε_y, (ii) increases with increasing strain-hardening exponent, (iii) has a size effect. By (iii) we mean that the inclusion radius enters into the critical load. To see this recall that the interface force law (33) is a function of $(\lambda_0 - 1)/\rho$ and $\lambda_0 - 1$ is the interface displacement normalized with respect to the inclusion radius (R_0). Then $R_0\rho$ $(= \delta)$ is a constitutive characteristic of the interface with the dimensions of length and ρ is the ratio of this property and the inclusion radius. Therefore, $(66)_2$ implies that larger inclusions will nucleate cavities prior to smaller ones, a fact which has been observed experimentally (Argon and Im, 1975; Goods and Brown, 1979; Fisher and Gurland, 1981a). Consider now the critical boundary circumferential strain for the finite sphere with smooth interface. Then $\varepsilon_1^* = c\varepsilon_0^* = c\rho$ which is given by $C\delta/R_0$. Associating this quantity with the nucleation strain, we find that ε_1^* (i) increases with increasing characteristic length parameter, (ii) decreases with increasing inclusion radius at fixed concentration and (iii) is independent of interface strength and matrix constitutive characteristics. Property (iii), which is not generally shared by other definitions of nucleation strain, is in large part due to the constraint of incompressibility and the specific geometry and loading considered. These aspects allow for the determination of the strain up to a multiplicative constant (the interface circumferential strain/normalized interface separation ε_0). Furthermore, because nucleation strain is here defined to be that strain at which non-symmetric deformation initiates it is to be expected that interfacial shear will strongly effect ε_1^*.

References

Abeyaratne, R., Horgan, C.O., 1985. Initiation of localized plane deformations at a circular cavity in an infinite compressible nonlinearly elastic medium. J. Elasticity 15, 243–256.

Argon, A.S., Im, J., 1975. Separation of second phase particles in spheroidized 1045 steel, cu-0.6 pct cr alloy, and maraging steel in plastic straining. Metall. Trans. 6A, 839–851.

Argon, A.S., Im, J., Safoglu, R., 1975. Cavity formation from inclusions in ductile fracture. Metall. Trans. 6A, 825–837.

Ball, J.M., 1982. Discontinuous equilibrium solutions and cavitation in nonlinear elasticity. Phil. Trans. R. Soc. Lond. A 306, 557–611.

Chung, D.-T., Horgan, C.O., Abeyaratne, R., 1987. A note on a bifurcation problem in finite plasticity related to void nucleation. Int. J. Solids Struct. 23, 983–988.

Corless, R.M., Gonnet, G.H., Hare, D.E.G., Jeffrey, D.J., 1993. Lambert's W function in Maple. MapleTech 3, 12–22.

Cox, T.B., Low, J.R., 1974. An investigation of the plastic fracture of AISI 4340 and 18 nickel-200 grade maraging steels. Metall. Trans. 5, 1457–1470.

Ferrante, J., Smith, J.R., Rose, J.H., 1982. Universal binding energy relations in metallic adhesion. In: Georges, J.M. (Ed.), Microscopic Aspects of Adhesion and Lubrication. Elsevier, Amsterdam, pp. 19–30.

Fisher, J.R., Gurland, J., 1981a. Void nucleation in spheroidized carbon steels. Part 1: experimental. Metal Sci. 15, 185–192.

Fisher, J.R., Gurland, J., 1981b. Void nucleation in spheroidized carbon steels. Part 2: model. Metal Sci. 15, 193–202.

Goods, S.H., Brown, L.M., 1979. The nucleation of cavities by plastic deformation. Acta Metall. 27, 1–15.

Hahn, G.T., Rosenfield, A.R., 1966. Effects of second-phase particles on ductility. Air Force Materials Laboratory Technical Report AFML-TR-65-409.

Horgan, C.O., Pence, T.J., 1989. Void nucleation in tensile dead-loading of a composite incompressible nonlinearly elastic sphere. J. Elasticity 21, 61–82.

Horgan, C.O., Polignone, D.A., 1995. Cavitation in nonlinear elastic solids: a review. Appl. Mech. Rev. 48, 471–485.

Levy, A.J., 1997. On the nucleation of cavities in planar elasticity. Phil. Trans. R. Soc. Lond. A 355, 2417–2458, Erratam: Phil. Trans. R. Soc. Lond. A 356, (1998) 669–670.

Levy, A.J., 1998. The affect of interfacial shear on cavity formation at an elastic inhomogeneity. J. Elasticity 50, 49–85.

Levy, A.J., Hardikar, K., 1999. The inclusion pair interaction problem with nonlinear interface. J. Mech. Phys. Solids 47, 1477–1508.

Levy, A.J., 2001. A finite strain analysis of cavity formation at a rigid inhomogeneity. J. Elasticity 64, 131–156.

Levy, A.J., 2002. Separation phenomena at the interface of a finitely deformed composite sphere. Int. J. Solids Struct. 39, 5813–5835.

Needleman, A., 1987. A continuum model for void nucleation by inclusion debonding. J. Appl. Mech. 54, 525–531.
Needleman, A., 1992. Micromechanical modelling of interfacial decohesion. Ultramicroscopy 40, 203–214.
Ogden, R.W., 1984. Non-Linear Elastic Deformations. Ellis Horwood, Chichester.
Rogers, H.C., 1960. The tensile fracture of ductile metals. AIME Trans. 218, 498–506.
Tanaka, K., Mori, T., Nakamura, T., 1970. Cavity formation at the interface of a spherical inclusion in a plastically deformed matrix. Phil. Mag. 21, 267–279.
Truesdell, C., Noll, W., 1965. The non-linear field theories of mechanics. In: Flugge, S. (Ed.), Encyclopedia of Physics, vol. lll/3. Springer Verlag, Heidelberg.